

A cannibalistic eco-epidemiological model with disease in predator population

Santosh Biswas¹ · Sudip Samanta² · Joydev Chattopadhyay²

Received: 18 January 2017 / Published online: 3 April 2017
© Korean Society for Computational and Applied Mathematics 2017

Abstract In this present article, we propose and analyze a cannibalistic predator–prey model with disease in the predator population. We consider two important factors for the dynamics of predator population. The first one is governed through cannibalistic interaction, and the second one is governed through the disease in the predator population via cannibalism. The local stability analysis of the model system around the biologically feasible equilibria are investigated. We perform global dynamics of the model using Lyapunov functions. We analyze and compare the community structure of the system in terms of ecological and disease basic reproduction numbers. The existence of Hopf bifurcation around the interior steady state is investigated. We also derive the sufficient conditions for the permanence and impermanence of the system. The study reveals that the cannibalism acts as a self-regulatory mechanism and controls the disease transmission among the predators by stabilizing the predator–prey oscillations.

Keywords Cannibalism · Disease transmission · Holling type II · Disease basic reproduction number · Lyapunov function · Hopf bifurcation

✉ Joydev Chattopadhyay
joydev@isical.ac.in

Santosh Biswas
sant_biswas@yahoo.in

Sudip Samanta
samanta.sudip.09@gmail.com

¹ Department of Mathematics, Jadavpur University, 188, Raja S. C. Mallik Road, Kolkata 700032, India

² Agricultural and Ecological Research Unit, Indian Statistical Institute, 203 B. T. Road, Kolkata 700108, India

Mathematics Subject Classification 92D40 · 92D30 · 92D25 · 34D20 · 34D23 · 34D10

1 Introduction

The dynamics of the predator–prey system is complex, and the complexity is enhanced in the presence of the disease either in prey or predator or *in both the populations*. We cannot ignore this factor as it is common in natural system and takes a major role for regulating community size. Disease in the predator species of the system leads to an array of interesting dynamics in ecological interaction [27–29, 32, 57]. Anderson and May [1] showed that infectious disease can destabilize the prey–predator interaction. Haderl and Freedman [26] studied an susceptible–infected (SI) model which is a modification of a Rosenzweig prey–predator system [48], and they found that the appearance of an infected steady state or periodic solution around the infected steady state is depending on some threshold value. Haque and Venturino [28] suggested that the disease in the predator population leads to a destabilizing effect on predator–prey population. The disease transmission in prey population, mostly occurred from contact with infected prey [1, 10, 12, 13, 24, 26, 31, 50–52, 56], whereas the predators are infected either through consumption of infected preys [1, 26, 55] or by contacts of infected predators [5, 57]. Although, cannibalism is another important disease transmission route in several species, such as Gill-associated virus [53] in *Penaeus mondon* and Spawner-isolated mortality virus [22] in *Pandalus platyceros* are transmitted among the species.

Cannibalism is a well-known and widespread phenomenon of consuming a member of its own species, and is common in many taxa ranging from invertebrates to mammals such as crustaceans, arachnids, zooplankton, insects, fishes, amphibians, reptiles, birds, etc. [16, 21]. It can be occurred for many factors such as density-dependent [6], density-independent [47], ecological and environmental [25]. For example, cannibalism among cephalopod is density dependent due to their aggressive predatory nature. It also depends on food availability and of the reproductive seasons [37]. In ecological interactions such as predation, competition, mutualism, parasitism and cannibalism can influence the evolution of interacting species [44]. In general, cannibalism acts as the fitness benefits to the species, such as increased survival, growth rate, longevity and fecundity [9]. It also has indirect benefits to the species for removing potential competitors, suppressing a population outbreak, and intra specific predators [21, 44]. Moreover, it could determine the population dynamics such as survival of the species [8], minimizes competition [21, 44], alter community structure (size [44, 61], age [15, 21]), evolution of life history [41] and decrease the rate of parasitism [34, 46, 58]. In the ecological system, the cannibalistic interacting dynamical models have been studied from various aspects such as regulating population size [15], controlling chaos [2], transmission route of diseases [9, 42], stabilization [4, 39, 54] and destabilization or chaotic effect on the species [30, 40]. Cannibalism can promote the dynamics of the population depending on the model and parameter values under which it is practiced [11, 14] in the sense of stability or instability aspects.

Cannibalism played a major role to increase disease transmission as well as mortality rates among the species in frog, fish and amphibians. Moreover, the transmission of viral host–pathogens occurred through cannibalism in aquatic systems [38]. Sometimes, cannibalism by multiple individuals on one prey (group cannibalism) is a necessary precondition in spreading diseases via cannibalism [49]. Notable exceptions arise in octopus species (*Enteroctopus megalocyathus*, *Octopus tehuelchus*) cannibalize their juveniles and female octopus (*Bathypolypus arcticus*) feed on their own nonviable or sick eggs to prevent the spread of infections [36,45,59]. This shows that cannibalism may work as a self-regulatory mechanism. In a study, Rudolf and Antonovics [49] have combined a cannibalistic predator–prey system with a model of classical susceptible–infected system and investigated the characteristic of disease transmission by cannibalism. Recently, Biswas et al. [3] proposed and analyzed a three-species prey–predator model with disease in predator population in which transmission of disease occurred through horizontal and vertical transmission. They also modified the model by considering that predator population is of cannibalistic nature. They observed that under some certain conditions, inclusion of cannibalism in predators can remove the disease propagation in predator species.

In general cannibalistic species with high size variation or high densities of conspecifics and/or low food resources, smaller individuals are more vulnerable to cannibalize by larger conspecifics [21,44]. So, cannibalistic type interaction depends on the size of both cannibal and victim but the precise relationship between the size of these two conspecific species is rarely known. Although there is an exception, when disease is present in conspecific species. In this case, the susceptible and infected individuals' conspecifics are not equally likely to be cannibalistic nature because the infected conspecifics are more prone to be cannibalized than the susceptible conspecific due to the infected conspecifics are weakened by the infection [23]. In this paper, we study a Lotka–Volterra type of predator–prey interaction model with disease present in the predator population. The predator population is cannibalistic in nature and the disease also transmitted in the predator population by cannibalism. In addition, functional response is one of the most crucial elements that describe the number of prey killed/ consumed by per individual predator per unit time. Many researchers suggested that type II response is the characteristic of predators. It determines the stability and bifurcation dynamics of the model. Usually, feeding rate of predator is saturated, so it is more realistic to consider prey dependence functional response Holling type II. Thus we incorporate Holling type II functional response to describe the predation strategy. The control of infectious disease transmission in a prey–predator system is one of the important challenging issues. The objective of this study is to find the condition(s) for which the disease could be prevented.

The paper is organized as follows. In Sect. 2, we describe the model formulation, which is based on some basic assumptions and hypothesis. Section 3 contains some preliminary results of existence, positivity and boundedness of solutions, and extinction criterion of the species. Section 4 performs an analysis of the model; in this section, we identify equilibria and their feasibility conditions, stability analysis around various steady states, from local as well as global point of view, and biological significance of threshold parameters and community structure. In this section, we also study the existence of Hopf bifurcation around the interior steady state of the system.

In Sect. 5, we find the conditions for the permanence and impermanence of the system. We performed extensive numerical simulations to validate our analytical findings and is presented in Sect. 6. Finally, the paper ends with a conclusion in Sect. 7.

2 Model formulation

We consider a system of two interacting species prey and predator with $x(t)$ is the numbers of prey species, $p(t)$ is the numbers of predator species at time t . We make the following assumptions for formulating the mathematical model of a prey–predator system.

1. In the absence of predation, the prey population $x(t)$ grows according to logistic fashion with an intrinsic growth rate $r \in R_+$ and environmental carrying capacity $k \in R_+$ such that

$$\frac{dx}{dt} = rx \left(1 - \frac{x}{k}\right). \quad (2.1)$$

2. In the presence of predation, we use the classical prey–predator model [48] which is of the form

$$\begin{aligned} \frac{dx}{dt} &= rx \left(1 - \frac{x}{k}\right) - \frac{\alpha_1 xp}{\gamma + x}, \\ \frac{dp}{dt} &= \frac{\alpha \alpha_1 xp}{\gamma + x} - dp. \end{aligned} \quad (2.2)$$

Here α_1 is the maximum predation rate for predator, α is the conversion rate of prey to predator, d is the constant natural death rate of predator. The functional response of predator follows Holling type II function with a half-saturation constant γ .

3. In the presence of disease in predator, the total predator population $p(t)$ is split into two classes, viz. susceptible predator whose population density is denoted by $y(t)$ and infected predator whose population density is denoted by $z(t)$. Thus $p(t) = y(t) + z(t)$ represents the total density of the predator at any time t .
4. The disease spreads among the predator species only, and the disease is not genetically inherited. The susceptible predator population becomes infected through the contact with the infectious predators at a rate λ , follows the mass action law λyz [1, 55, 57].
5. The susceptible and infected predators consume the prey with different predation rates, denoted respectively by α_1 and α_2 , with $\alpha_1 > \alpha_2$. This is due to the fact that the susceptible predators are more efficient to catch the prey than the infected ones, weakened by the infection. It is assumed that infected predators do not recover from the disease. Considering the above assumptions, the model (2.2) takes the following form

$$\begin{aligned} \frac{dx}{dt} &= rx \left(1 - \frac{x}{k}\right) - \frac{(\alpha_1 y + \alpha_2 z)x}{\gamma + x}, \\ \frac{dy}{dt} &= \frac{\alpha(\alpha_1 y + \alpha_2 z)x}{\gamma + x} - \lambda yz - dy, \\ \frac{dz}{dt} &= \lambda yz - (d + e)z, \end{aligned} \tag{2.3}$$

where e is the additional disease-related mortality rate.

6. We assume that, cannibalism is present in the predator species and the disease also spreads among the predator population via cannibalism.
7. In the presence of cannibalism, the susceptible and infected predators are reduced with two different rates $\beta\sigma$ and σ ($0 < \beta < 1$). This is due to the fact that both the susceptible and infected predator populations are not equally likely to be cannibalized. In nature, the infected predators are more prone to be cannibalized than healthy ones as infected predators are weakened by the infection [23].
8. The susceptible population is increased at different conversion rates c_1 and c_1 due to resources gained through cannibalism. The dimensionless quantities c_1 and c_2 are conversion rates to the susceptible predator for the species y and z respectively. It is assumed that a predator cannot produce more than one susceptible predator per predator consumed, that is, $c_1, c_2 < 1$.
9. The susceptible predator becomes infected via cannibalistic transmission and this process is assumed to follow the simple law of mass action with σlf measuring the force of infection. Here σ is a non-negative constant, and defined by the number of predators killed and consumed per predator per time or attack rate due to cannibalism. l is the probability of transmission for cannibalistic interaction and f is the number of predators sharing one conspecific predator.

On the basis of the above assumptions we propose the following mathematical model,

$$\begin{aligned} \frac{dx}{dt} &= rx \left(1 - \frac{x}{k}\right) - \frac{(\alpha_1 y + \alpha_2 z)x}{\gamma + x}, \\ \frac{dy}{dt} &= \frac{\alpha(\alpha_1 y + \alpha_2 z)x}{\gamma + x} + c_1\sigma(\beta y + z)y \\ &\quad + c_2\sigma(\beta y + z)z - \sigma(\beta y + z)y - \sigma l f yz - \lambda yz - dy, \\ \frac{dz}{dt} &= \lambda yz + \sigma l f yz - \sigma(\beta y + z)z - (d + e)z. \end{aligned} \tag{2.4}$$

System (2.4) is to be analyzed with the following initial conditions

$$x(0) > 0, \quad y(0) > 0, \quad z(0) > 0.$$

Since all the parameters of (2.4) are non-negative, the right hand side is a smooth function of the variables x, y, z in the positive region $E = \{(x, y, z); x, y, z \in R_+\}$.

3 Some preliminary results

3.1 Existence, positive invariance

Proposition 1 *Every solution of the system (2.4) with positive initial values exists and is unique in the interval $[0, \infty)$ and $x(t) > 0, y(t) > 0, z(t) > 0, \forall t \geq 0$.*

Proof Denoting $Z \equiv (x, y, z)^T$ and $F(Z) = [F_1(Z), F_2(Z), F_3(Z)]^T$ such that $F_1 = rx(1 - \frac{x}{k}) - \frac{(\alpha_1 y + \alpha_2 z)x}{\gamma + x}, F_2 = \frac{\alpha(\alpha_1 y + \alpha_2 z)x}{\gamma + x} + c_1 \sigma(\beta y + z)y + c_2 \sigma(\beta y + z)z - \sigma(\beta y + z)y - \sigma l f y z - \lambda y z - d y, F_3 = \lambda y z + \sigma l f y z - \sigma(\beta y + z)z - (d + e)z$. Then system (2.4) can be written in the form $\dot{Z} = F(Z)$, where $F : C_+ \rightarrow R_+^3$ with $Z(0) = Z_0 \in R_+^3, F_i \in C^\infty(R_+)$, for $i = 1, 2, 3$. Thus, vector function F is a locally Lipschitzian and completely continuous function of the variables x, y, z in the positive octant $E = \{(x(t), y(t), z(t)); x > 0, y > 0, z > 0\}$. Applying the lemma in [60], we can say that any solution (x, y, z) of the system (2.4) with positive initial values exists and is unique in the interval $[0, c]$, $\forall t \geq 0$, where c is a finite positive real number. \square

3.2 Boundedness

Proposition 2 *All feasible solutions of the system (2.4) are uniformly bounded in the region*

$$E_\varepsilon = \left\{ (x, y, z) \in R_+^3 : x + y + z \leq \frac{\widehat{k}(r + 1)}{m} + \varepsilon \right\}.$$

Proof Let $V(x, y, z) = x + y + z$, then we have

$$\begin{aligned} \frac{dV}{dt} &= rx \left(1 - \frac{x}{k} \right) - (1 - \alpha) \frac{x(\alpha_1 y + \alpha_2 z)}{\sigma + x} - \sigma(\beta y + z)[(1 - c_1)y + (1 - c_2)z] \\ &\quad - dy - (d + e)z \text{ (by using (2.4))} \\ &\leq rx \left(1 - \frac{x}{k} \right) - dy - (d + e)z \text{ (since } \alpha, c_1, c_2 < 1) \\ &= x \left[r \left(1 - \frac{x}{k} \right) + 1 \right] - x - dy - (d + e)z \\ &\leq x(r + 1) - x - dy - (d + e)z. \end{aligned}$$

In particular, $\limsup_{t \rightarrow \infty} x(t) \leq \widehat{k}$ since $\frac{dx}{dt} \leq rx(1 - \frac{x}{k})$, where $\widehat{k} = \max\{x(0), k\}$. Thus, $x(t)$ is bounded and defined on $[0, \infty) \forall t \geq 0$.

Hence, $\frac{dV}{dt} + mV \leq \widehat{k}(r + 1)$, where $m = \min\{1, d, d + e\}$.

Now applying the theory of differential inequality we get,

$$0 < V(x, y, z) \leq \frac{\widehat{k}(r + 1)}{m} + e^{-mt} V(x(0), y(0), z(0))$$

which implies $0 < V(x, y, z) \leq \frac{\widehat{k}(r+1)}{m}$ as $t \rightarrow \infty$.

So all the solutions of (2.4) with positive initial values are confined in the region

$$E_\varepsilon = \left\{ (x, y, z) \in \mathbb{R}_+^3 : x + y + z \leq \frac{\widehat{k}(r + 1)}{m} + \varepsilon \right\} \text{ for any } \varepsilon > 0.$$

Hence the result.

3.3 Extinction criterion

Proposition 3 *If $\alpha_1 y(t) \geq r(\gamma + \widehat{k})$, then $\lim_{t \rightarrow \infty} x(t) = 0$. If $\{\lambda + \sigma lf - \sigma \beta\}y(t) \leq (d + e)$, then $\lim_{t \rightarrow \infty} z(t) = 0$. If $\alpha \alpha_1 \leq d$, then $\lim_{t \rightarrow \infty} y(t) = 0$.*

Proof

$$\frac{dx}{dt} = rx \left(1 - \frac{x}{k} \right) - \frac{(\alpha_1 y + \alpha_2 z)x}{\gamma + x} \leq x \left(r - \frac{\alpha_1 y}{\gamma + x} \right)$$

Therefore, $x(t) = x(t_0) \exp \left\{ \int_{t_0}^t \left(r - \frac{\alpha_1 y(\xi)}{\gamma + x(\xi)} \right) d\xi \right\}$

$$x(t) \leq x(t_0) \exp \left\{ \int_{t_0}^t \left(r - \frac{\alpha_1 y(\xi)}{\gamma + \widehat{k}} \right) d\xi \right\}, \text{ since } \lim_{t \rightarrow \infty} \sup x(t) \leq \widehat{k}.$$

Thus if $\alpha_1 y(t) \geq r(\gamma + \widehat{k})$, then $\lim_{t \rightarrow \infty} x(t) = 0$.

$$\frac{dz}{dt} = \lambda yz + \sigma l f yz - \sigma(\beta y + z)z - (d + e)z \leq z\{\lambda + \sigma l f - \sigma \beta\}y - (d + e)z$$

$$z(t) \leq z(t_0) \exp \left[\int_{t_0}^t (\lambda + \sigma l f - \sigma \beta)y(\xi) - (d + e) d\xi \right].$$

Hence $\lim_{t \rightarrow \infty} z(t) = 0$ provided $(\lambda + \sigma l f - \sigma \beta)y(t) \leq (d + e)$.

Again from second and third equations of the system (2.4) we have

$$\begin{aligned} \frac{dy}{dt} + \frac{dz}{dt} &= \frac{\alpha(\alpha_1 y + \alpha_2 z)x}{\gamma + x} \\ &\quad - \sigma(1 - c_1)(\beta y + z)y - \sigma(1 - c_2)(\beta y + z)z - d(y + z) - ez \end{aligned}$$

$$\begin{aligned} \frac{d}{dt}(y + z) &\leq \frac{\alpha \alpha_1 (y + z)x}{\gamma + x} - d(y + z) \\ &\leq (\alpha \alpha_1 - d)(y + z). \end{aligned}$$

Therefore, $y(t) + z(t) = [y(t_0) + z(t_0)] \exp \left\{ \int_{t_0}^t (\alpha \alpha_1 - d) d\xi \right\} \leq [y(t_0) + z(t_0)] \exp \{(\alpha \alpha_1 - d)(t - t_0)\}$.

Thus $\lim_{t \rightarrow \infty} \{y(t) + z(t)\} = 0$ provided $\alpha \alpha_1 \leq d$.

Again $\lim_{t \rightarrow \infty} z(t) = 0$ hence $\lim_{t \rightarrow \infty} y(t) = 0$.

4 Qualitative analysis of the model

4.1 Equilibria and their existence

The system (2.4) has four equilibrium points. $B_0(0, 0, 0)$ is the trivial equilibrium point. The predator free axial equilibrium point is $B_1(k, 0, 0)$. Disease-free planar equilibrium point is $B_2(x_2, y_2, 0)$, where $y_2 = \frac{1}{\sigma\beta(1-c_1)}(\frac{\alpha\alpha_1x_2}{\gamma+x_2} - d)$ and x_2 is the unique positive real root of the cubic equation

$$a_0x_2^3 + 3a_1x_2^2 + 3a_2x_2 + a_3 = 0, \tag{4.1}$$

where $a_0 = \frac{r\sigma\beta(1-c_1)}{k}$, $3a_1 = (\frac{2\gamma}{k} - 1)r\sigma\beta(1-c_1)$, $3a_2 = \alpha\alpha_1^2 - \alpha_1d - 2r\sigma\beta\gamma + \frac{r\sigma\beta\gamma^2}{k}$ and $a_3 = -\{r\sigma\beta\gamma^2(1-c_1) + d\alpha_1\gamma\}$.

The above Eq. (4.1) has exactly one real positive root if $G^2 + 4H^3 > 0$ with $G = a_0^2a_3 - 3a_0a_1a_2 + 2a_1^3$ and $H = a_0a_2 - a_1^2$. If ξ_0 denotes one of the cubic root of $\frac{1}{2}[-G + \sqrt{G^2 + 4H^3}]$ and by Cardano’s method, the root is $\frac{1}{a_0}[\xi_0 - a_1 - \frac{H}{\xi_0}]$. If $G^2 + 4H^3 = 0$ then the Eq. (4.1) has two equal roots and the condition $G^2 + 4H^3 < 0$ together with $H < 0$ gives three distinct real roots. B_2 denotes the one and only one positive disease-free planar equilibrium point of the system (2.4) but when the Eq. (4.1) has three distinct positive roots, so we can get three different equilibrium points, denoting them by $B_2^{(i)}$, $B_2^{(ii)}$ and $B_2^{(iii)}$.

The interior equilibrium point is given by $B_*(x_*, y_*, z_*)$, where $z_* = \frac{1}{\alpha}[(\lambda + \sigma lf - \sigma\beta)y_* - (d + e)]$, x_* and y_* are the positive roots of the following set of two equations

$$\begin{aligned} b_1x^2 + b_2x + b_3y + b_4 &= 0, \\ d_1y^2 + d_2\frac{xy}{\gamma+x} + d_3y + d_4\frac{x}{\gamma+x} + d_5 &= 0, \end{aligned} \tag{4.2}$$

where $b_1 = \frac{r}{k}$, $b_2 = r(\frac{\gamma}{k} - 1)$, $b_3 = \alpha_1 + \alpha_2(fl - \beta + \frac{\lambda}{\sigma})$, $b_4 = -\{r\gamma + \alpha_2(d + e)\}$, $d_1 = c_2(\lambda + \sigma lf - \sigma\beta)^2 + (c_1\sigma - \sigma - \sigma lf - \lambda)(\lambda + \sigma lf - \sigma\beta) + (c_1\sigma\beta - \sigma\beta)\sigma$, $d_2 = \alpha[\alpha_1\sigma + \alpha_2(\lambda + \sigma lf - \sigma\beta)]$, $d_3 = -[(c_1\sigma - \sigma - \sigma lf - \lambda)(d + e) + 2c_2(d + e)(\lambda + \sigma lf - \sigma\beta) + \sigma d]$, $d_4 = -\alpha\alpha_2(d + e)$ and $d_5 = c_2(d + e)^2$.

The equilibrium points B_0, B_1 always exist. The equilibrium point B_2 is admissible if $\frac{\alpha\alpha_1x_2}{\gamma+x_2} > d$. The existence condition of interior equilibrium is $y_* > \frac{(d+e)}{\lambda+\sigma lf-\sigma\beta}$.

4.2 Stability analysis

In this section, we deal with local and global stability of the system (2.4) around each of the equilibria. The Jacobian matrix J of the system (2.4) at any arbitrary point (x, y, z) is given by

$$J \equiv \begin{bmatrix} r(1 - 2\frac{\gamma}{k}) - \frac{(\alpha_1y + \alpha_2z)}{\gamma+x} + \frac{(\alpha_1y + \alpha_2z)x}{(\gamma+x)^2} & -\frac{\alpha_1x}{\gamma+x} & -\frac{\alpha_2x}{\gamma+x} \\ \frac{\alpha(\alpha_1y + \alpha_2z)}{\gamma+x} - \frac{\alpha(\alpha_1y + \alpha_2z)x}{(\gamma+x)^2} & \frac{\alpha\alpha_1x}{\gamma+x} + c_1\sigma(2\beta y + z) + c_2\sigma\beta z & \frac{\alpha\alpha_2x}{\gamma+x} + c_1\sigma y + c_2\sigma(\beta y + 2z) \\ 0 & -\sigma(2\beta y + z) - \sigma lfz - \lambda z - d & -\sigma y - \sigma lf y - \lambda y \\ & \lambda z + \sigma lfz - \sigma\beta z & \lambda y + \sigma lf y - \sigma(\beta y + 2z) - (d + e) \end{bmatrix}.$$

4.2.1 The behavior of the system around $B_0(0, 0, 0)$

Let J_0 be the Jacobian matrix of the system (2.4) at equilibrium point B_0 , then eigenvalues at B_0 are $r, -d$ and $-(d + e)$. Then there exists a two-dimensional differential stable manifold in yz -plane and one-dimensional unstable manifold in x -axis. Thus, the system (2.4) is always unstable around B_0 .

4.2.2 The behavior of the system around $B_1(k, 0, 0)$

Theorem 1 (a) The axial equilibrium point $B_1(k, 0, 0)$ of the system (2.4) is locally asymptotically stable if $R_{01} < 1$, where $R_{01} = \frac{\alpha\alpha_1k}{d(\gamma+k)}$.
 (b) B_1 is globally asymptotically stable if $d \geq \alpha_1(\alpha + k)$.

Proof (a) The eigenvalues associated with the Jacobian matrix J_1 around the axial equilibrium point B_1 are $-r, -(d + e)$ and $\frac{\alpha\alpha_1k}{\gamma+k} - d$. Therefore, the system is locally asymptotically stable if $R_{01} < 1$.

(b) Let $\mathcal{R}_{+x}^3 = \{(x, y, z) \in \mathbb{R}_+^3 : x > 0, y \geq 0, z \geq 0\}$ and consider a positive definite function $\mathcal{Y} : \mathcal{R}_{+x}^3 \rightarrow \mathbb{R}$ about $B_1(k, 0, 0)$, given by

$$\mathcal{Y}(x, y, z) = \frac{1}{2}(x - k)^2 + y + z.$$

The derivative of \mathcal{Y} w.r.t time t along the solution of the system (2.4), we get

$$\begin{aligned} \dot{\mathcal{Y}} &= (x - k) \left[rx \left(1 - \frac{x}{k} \right) - \frac{(\alpha_1 y + \alpha_2 z)x}{\gamma + x} \right] + \frac{\alpha(\alpha_1 y + \alpha_2 z)x}{\gamma + x} \\ &\quad + c_1 \sigma(\beta y + z)y + c_2 \sigma(\beta y + z)z - \sigma(\beta y + z)y - dy \\ &\quad - \sigma(\beta y + z)z - (d + e)z \\ &\leq -\frac{rx(x - k)^2}{k} - \frac{(\alpha_1 y + \alpha_2 z)x^2}{\gamma + x} + k(\alpha_1 y + \alpha_2 z) + \alpha(\alpha_1 y + \alpha_2 z) \\ &\quad - \sigma(1 - c_1)(\beta y + z)y - \sigma(1 - c_2)(\beta y + z)z - d(y + z) - ez \\ &= -\frac{rx(x - k)^2}{k} - \frac{(\alpha_1 y + \alpha_2 z)x^2}{\gamma + x} - \sigma(1 - c_1)(\beta y + z)y \\ &\quad - \sigma(1 - c_2)(\beta y + z)z - (d - \alpha_1 k - \alpha\alpha_1)y - (d + e - \alpha_2 k - \alpha\alpha_2)z \end{aligned}$$

≤ 0 , if $d \geq \max\{\alpha_1(\alpha + k), \alpha_2(\alpha + k) - e\} = \alpha_1(\alpha + k)$ (since $\alpha_1 > \alpha_2$ and $c_1, c_2 < 1$); and $\dot{\mathcal{Y}} = 0$ at $(x, y, z) = (k, 0, 0)$. Hence, the equilibrium point B_1 is globally asymptotically stable for $d \geq \alpha_1(\alpha + k)$.

4.2.3 The behavior of the system around $B_2(x_2, y_2, 0)$

Theorem 2 (a) The disease-free equilibrium point $B_2(x_2, y_2, 0)$ of the system (2.4) is locally asymptotically stable if $R_{02} < 1, \sigma > \sigma^{[2]}$ and $r > r^{[2]}$, where $R_{02} = \frac{(\lambda + \sigma I_f)y_2}{\sigma\beta y_2 + d + e}, \sigma^{[2]} = \frac{x_2}{\beta(1 - c_1)y_2} \left[\frac{\alpha y_2}{(\gamma + x_2)^2} - \frac{r}{k} \right], r^{[2]} = \frac{\alpha k y_2}{(\gamma + x_2)^2}$.

(b) If $r\gamma + (1 - c_1)\sigma\beta \geq \alpha_1$, then local stability of the axial equilibrium point B_2 ensures its global stability in the region \mathcal{R}_+^2 of xy -plane, where $\mathcal{R}_+^2 = \{(x, y); x > 0, y > 0\}$.

Proof (a) The Jacobian matrix around B_2 is given by

$$J_2 = \begin{bmatrix} -\frac{rx_2}{k} + \frac{\alpha_1 y_2 x_2}{(\gamma + x_2)^2} & -\frac{\alpha_1 x_2}{\gamma + x_2} & -\frac{\alpha_2 x_2}{\gamma + x_2} \\ \frac{\alpha \alpha_1 \gamma y_2}{(\gamma + x_2)^2} & \sigma\beta(c_1 - 1)y_2 & \frac{\alpha \alpha_2 x_2}{\gamma + x_2} + c_1 \sigma y_2 + c_2 \sigma \beta y_2 - \sigma y_2 - \sigma l f y_2 - \lambda y_2 \\ 0 & 0 & (\lambda + \sigma l f - \sigma\beta)y_2 - (d + e) \end{bmatrix}.$$

The characteristic roots of the Jacobian matrix J_2 are $(\lambda + \sigma l f - \sigma\beta)y_2 - (d + e)$ and other two roots are given by

$$\mu^2 + \pi_1 \mu + \pi_2 = 0,$$

where

$$\begin{aligned} \pi_1 &= \frac{rx_2}{k} + \sigma\beta(1 - c_1)y_2 - \frac{\alpha_1 y_2 x_2}{(\gamma + x_2)^2}, \\ \pi_2 &= \sigma\beta(1 - c_1)x_2 y_2 \left[\frac{r}{k} - \frac{\alpha_1 y_2}{(\gamma + x_2)^2} \right] + \frac{\alpha \alpha_1^2 x_2 y_2}{(\gamma + x_2)^3}. \end{aligned}$$

Hence, the system is locally asymptotically stable around B_2 if $R_{02} < 1, \sigma > \sigma^{[2]}$ and $r > r^{[2]}$.

(b) For the equilibrium point $B_2(x_2, y_2, 0)$, we consider $\varpi(x, y) = \frac{\gamma + x}{x^2 y}, \varphi_1(x, y) = rx(1 - \frac{x}{k}) - \frac{\alpha_1 y x}{\gamma + x}, \varphi_2(x, y) = \frac{\alpha \alpha_1 y x}{\gamma + x} + c_1 \sigma \beta y^2 - \sigma \beta y^2 - dy$ and

$$\mathcal{D}(x, y) = \frac{\partial(\varphi_1 \varpi)}{\partial x} + \frac{\partial(\varphi_2 \varpi)}{\partial y}.$$

Thus, $\varpi(x, y) > 0 \forall x > 0, y > 0$. Then we can get

$$\begin{aligned} \mathcal{D} &= -\frac{r\gamma}{x^2} - \frac{r}{yk} - \frac{1}{x^2}(\sigma\beta - c_1\sigma\beta - \alpha_1) - \frac{1}{x}(1 - c_1)\sigma\beta \\ &= -\frac{1}{x^2}[r\gamma + \sigma\beta(1 - c_1) - \alpha_1] - \frac{r}{yk} \\ &\quad - \frac{1}{x}(1 - c_1)\sigma\beta < 0 \text{ if } r\gamma + (1 - c_1)\sigma\beta \geq \alpha_1. \end{aligned}$$

By *Bendixson–Dulac* criteria, we observe that if $r\gamma + (1 - c_1)\sigma\beta \geq \alpha_1$, then \mathcal{D} does not change sign and is not identically zero in the interior of first quadrant of xy -plane. Therefore, the system (2.4) has no periodic solution in the positive quadrant of xy -plane. Thus, if B_2 is locally asymptotically stable, then it will be globally asymptotically stable in the region \mathcal{R}_+^2 of xy -plane.

4.2.4 Biological significance of threshold parameters and community structure

We discuss the biological significance of threshold parameters obtained from local stability analysis of axial and planar equilibrium points. Each threshold parameter has clear and distinct biological meanings. The community composition of the model system can be completely explained in terms of *ecological* and *disease* basic reproduction numbers. We define the threshold parameter R_{01} by

$$R_{01} = \frac{\alpha\alpha_1k}{d(\gamma + k)}$$

which determines the local stability of the axial equilibrium point $B_1(k, 0, 0)$. This expression can be considered as the *disease-free demographic reproduction number*. The term $\frac{\alpha\alpha_1k}{\gamma+k}$ is the birth rate of predator and $\frac{1}{d}$ is the mean lifespan of a healthy predator. Subsequently, the above two relations together give the mean number of newborn predators by a predator. So, R_{01} is also interpreted as the *ecological basic reproduction number*. We also note that Pielou [43] first formulated this term and explained as the average number of prey converted to predator biomass in a course of predator’s life span [31]. The condition $R_{01} < 1$ implies that the predator goes to extinct and only the prey populations survive in the predator-free system.

For local stability of the system at the disease-free planar equilibrium point $B_2(x_2, y_2, 0)$ is related to a basic reproduction number R_{02} , where

$$R_{02} = \frac{(\lambda + \sigma lf)y_2}{\sigma\beta y_2 + d + e}.$$

Here, the term $(\lambda + \sigma lf)y_2$ is the infection rate of a new infective predator appearing in a totally susceptible predator population in the absence of the disease infection and $\sigma\beta y_2 + d + e$ is the removal rate of infected predator population around B_2 . So, R_{02} is interpreted as *disease basic reproduction number* in the predator population. The parameter R_{02} , together with $\frac{\sigma^{[2]}}{\sigma}$ and $\frac{r^{[2]}}{r}$ govern whether disease is wipeout from the system. If $R_{02} < 1$, $\sigma > \sigma^{[2]}$ and $r > r^{[2]}$, the infection will die out in the long run i.e., the disease-free steady-state B_2 is locally stable on the xy -plane. When $R_{02} > 1$, clearly the disease-free steady state loses its local stability, and the infection is able to spreads among the predators. Thus, there exists a stable interior steady-state in which disease is always present in the predator population.

4.2.5 The behavior of the system around $B_*(x_*, y_*, z_*)$

Theorem 3 (a) *The interior equilibrium point $B_*(x_*, y_*, z_*)$ of the system (2.4) is locally asymptotically stable if $\Theta_1 > 0$, $\Theta_3 > 0$ and $\Theta_1\Theta_2 - \Theta_3 > 0$, where Θ_i ’s are prescribe in the proof of the theorem.*

(b) *If*

$$I. \frac{r}{k} \geq \max \left[\frac{\alpha_1 y_* + \alpha_2 z_*}{\gamma(\gamma + x_*)}, \frac{\alpha_1 y_* + \alpha_2 z_*}{\gamma(\gamma + x_*)} + \frac{1}{4\sigma(1 - c_1)\beta} \left(\frac{\alpha_1}{\gamma} \right)^2 \right], \tag{4.3}$$

$$\begin{aligned}
 \text{II. } \alpha_1 \geq \max & \left[\sqrt{\frac{\alpha\gamma}{\gamma+x_*} \frac{\alpha_2 z_*}{y}}, \frac{\alpha\alpha_2\gamma z_*}{\left(1 - \frac{\alpha\gamma}{\gamma+x_*}\right)(\gamma+x)(\gamma+x_*)y} \right. \\
 & + \frac{2r(\gamma+x)^2}{\alpha_2 k \left(1 - \frac{\alpha\gamma}{\gamma+x_*}\right)} \{ \sigma(1-c_1) + \sigma\beta(1-c_2) \}, \\
 & \left. \frac{\alpha\alpha_2\gamma z_*}{\left(1 - \frac{\alpha\gamma}{\gamma+x_*}\right)(\gamma+x_*)y} + \frac{2\alpha_2 \left\{ \sigma(1-c_1)\beta + \frac{c_2\sigma z_*^2}{y_*y} + \frac{\alpha\alpha_2 x_* z_*}{(\gamma+x_*)y_*y} \right\}}{\left(1 - \frac{\alpha\gamma}{\gamma+x_*}\right) \{ \sigma(1-c_1) + \sigma\beta(1-c_2) \}} \right], \tag{4.4}
 \end{aligned}$$

$$\text{III. } \sigma(1-c_1) + \sigma\beta(1-c_2) > c_2\sigma \frac{z}{y} + c_2\sigma \frac{z_*}{y} + \frac{\alpha\alpha_2 x}{(\gamma+x)y} \quad \text{and} \tag{4.5}$$

$$\text{IV. } \gamma \geq \frac{\alpha_1(\gamma+x)y}{\alpha\alpha_2 z_*} \tag{4.6}$$

then, the existence of positive interior equilibrium point B_* of the system (2.4) implies its global stability around the positive interior equilibrium point.

Proof See Appendix 1. □

We have also summarized the existence, local stability and global stability criteria of the equilibrium points of the system (2.4) in Table 1.

Remark 1 The system (2.4) is stable around the predator-free equilibrium (B_1) if $R_{01} < 1$ and becomes unstable if $R_{01} > 1$. Therefore, the predator-free equilibrium undergoes a transcritical bifurcation at $R_{01} = 1$. Furthermore, the system (2.4) is stable around the disease-free equilibrium (B_2) if $R_{02} < 1$ and becomes unstable if $R_{02} > 1$ and the disease starts to persist in the system. Therefore, another transcritical bifurcation occurs at $R_{02} = 1$.

Hopf bifurcation analysis We know that, the steady state B_* will lose its stability when one of the parameters changes. We choose σ , the cannibalistic attack rate as the bifurcation parameter. We shall find out the conditions for which the solution of the system (2.4) enters into Hopf bifurcation on some submanifold in parameter space

Table 1 Community composition and stability of equilibria

| Equilibrium pt. | Existence criterion | LAS criterion | Sufficient conditions for GAS |
|----------------------|---|---|--|
| $B_0(0, 0, 0)$ | Always exists | Always unstable | Always unstable |
| $B_1(k, 0, 0)$ | Always exists | $R_{01} < 1$ | $\alpha_1(\alpha + k) \leq d$ |
| $B_2(x_2, y_2, 0)$ | $\frac{\alpha\alpha_1 x_2}{\gamma+x_2} > d$ | $R_{02} < 1, \sigma > \sigma^{[2]}$ and $r > r^{[2]}$ | $r\gamma + (1 - c_1)\sigma\beta \geq \alpha_1$ |
| $B_*(x_*, y_*, z_*)$ | $y_* > \frac{(d+e)}{\lambda+\sigma l f - \sigma\beta}$ and Eq. (4.2) | $\Theta_1 > 0, \Theta_3 > 0$ and $\Theta_1\Theta_2 - \Theta_3 > 0$ | Eqs. (4.3)–(4.6) |

corresponding to fixed $\sigma = \sigma^*$. Now the system (2.4) will admit a Hopf bifurcation around the interior steady state B_* follows the theorem is stated at below.

Theorem 4 *If cannibalistic attack rate σ passes through the critical value σ^* and the following conditions hold:*

- (i) $\Theta_1(\sigma^*) > 0, \Theta_2(\sigma^*) > 0;$
- (ii) $\Theta_3(\sigma^*) = \Theta_1(\sigma^*)\Theta_2(\sigma^*);$
- (iii) $\dot{\Theta}_3(\sigma^*) > [\Theta_1(\sigma^*)\Theta_2(\sigma^*)]'$,

then the system (2.4) undergoes a Hopf bifurcation at the interior equilibrium point B_* .

Proof See Appendix 2. □

5 Permanence and impermanence

Here we wish to discuss the permanence and impermanence of the system (2.4) with positive initial conditions. Biologically, permanence of the system means the coexistence of all species of the system in future time. Mathematically, permanence of the system means that strictly positive solutions having no omega limit points on the boundary of the non negative cone.

Theorem 5 *Suppose that $R_{01} > 1$, and if there exists a finite number of periodic solutions $x = \varphi_q(t), y = \psi_q(t), q = 1, 2, \dots, n$, in the xy -plane, then system (2.4) is uniformly persistent provided for each periodic solutions of period T ,*

$$\zeta_q = -(d + e) + \frac{1}{T} \int_0^T [(\lambda + \sigma l f - \sigma \beta)\varphi_q - \sigma \psi_q] dt > 0, \forall q = 1, 2, \dots, n.$$

Proof See Appendix 3. □

Before starting our theorem on impermanence of the system (2.4), we give a definition of impermanence of the system. Let $\kappa = (\kappa_1, \kappa_2, \kappa_3)$ be the population vector, $\mathcal{B} = \{\kappa : \kappa_i > 0 \forall i = 1, 2, 3\}$, $\partial\mathcal{B}$ is the boundary of \mathcal{B} , and $d_0(\cdot, \cdot)$ is the distance in R_+^3 .

Consider the system of equations, given by

$$\dot{\kappa} = f_j(\kappa) \quad j = 1, 2, 3,$$

where $f_j : R_+^3 \rightarrow R$ and $f_j \in C^1$.

Let $\kappa(t)$ be a solution with initial value $\kappa(0) = \kappa_0$, then the semi orbit γ^+ is defined by the set $\{\kappa(t) : t > 0\}$.

According to Hutson and Law (1985), the above system is said to be impermanent iff there is an $\kappa \in \mathcal{B}$ such that $\lim_{t \rightarrow \infty} d_0 < \kappa(t), \partial\mathcal{B} > = 0$. Thus, a community is impermanent if there is at least one semi-orbit which tends to the boundary.

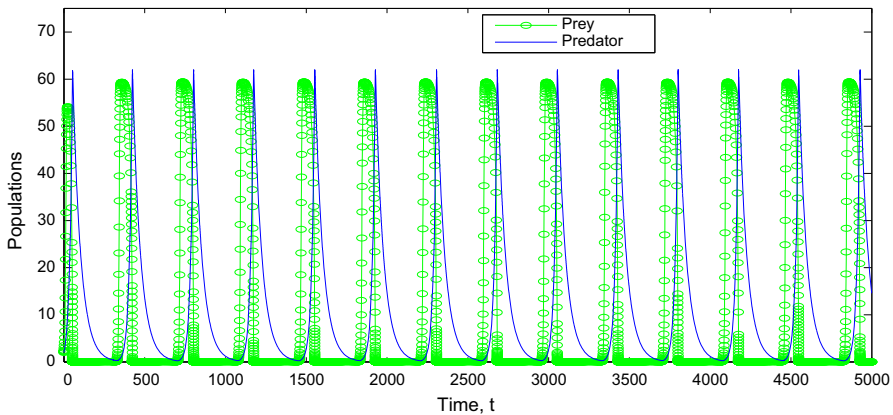


Fig. 1 The figure depicts the solution of the system (2.4) in the absence of disease and cannibalism for parameter values are $r = 0.4$; $k = 60.0$; $\alpha_1 = 0.2$; $\alpha_2 = 0.1$; $\alpha = 0.4$; $\gamma = 0.7$; $d = 0.02$; $e = 0.01$; $\lambda = 0.0$; $\sigma = 0.0$

Theorem 6 *The system (2.4) is impermanent if $R_{01} < 1$ or $R_{02} < 1$.*

Proof The equilibrium point B_1 is locally stable on the boundary when $R_{01} < 1$. The condition $R_{02} < 1$ implies that B_2 is a saturated fixed point on boundary. Thus, there exists at least one orbit in positive cone that converges to the boundary [33]. Hence the system (2.4) is impermanent [35].

6 Numerical simulations

In this section, we perform numerical simulations of the system (2.4) by using 4th order Runge–Kutta method [7] in Matlab 7.6 software. *The numerical simulation can also be performed by the multistage Adomian decomposition method as another efficient alternative [17–20].* Here cannibalistic attack rate σ , conversion rates c_1 , c_2 due to cannibalism, disease transmission rate λ and conversion efficiency α of predator are important parameters under investigation. The main purpose of this section is to study the dynamical behavior of the model for a wide range of above parameter values. To validate the analytical findings of the model, we choose a set of biologically feasible hypothetical parameter values $r = 0.4$; $K = 60.0$; $\alpha_1 = 0.2$; $\alpha_2 = 0.1$; $\alpha = 0.4$; $\gamma = 0.7$; $d = 0.02$; $e = 0.01$; $\lambda = 0.004$; $\sigma = 0.005$, $c_1 = 0.3$; $c_2 = 0.2$; $\beta = 0.3$; $l = 0.01$; $f = 10.0$ (see Table 2).

It is observed from Fig. 1 that the prey and predator populations coexist with oscillatory nature in the absence of disease and cannibalism ($\lambda = 0$, $\sigma = 0$). But Fig. 2 demonstrates that in the absence of cannibalism, the disease spreads among the predators for a certain disease transmission rate $\lambda = 0.004$.

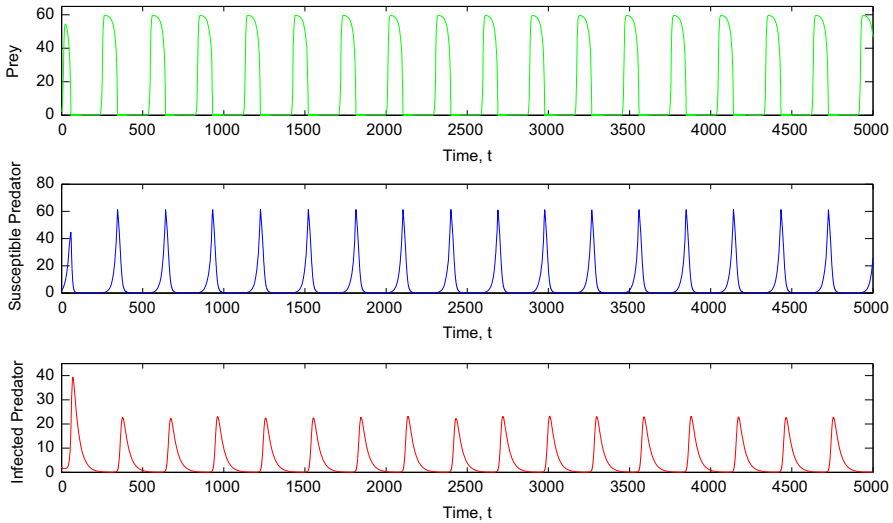


Fig. 2 The figure depicts the solution of the system (2.4) in the absence of cannibalism for $\lambda = 0.004$ and other parameter values as in Fig. 1

6.1 Role of cannibalistic attack rate σ

We have already stated that cannibalistic attack rate among the predators has a significant impact on the dynamics of the system. We like to observe the dynamics of the system (2.4) for changing the cannibalistic attack rate σ . Figure 2 shows all species coexist in oscillatory dynamics for $\sigma = 0$ and the other parameters remain same as in Table 2. Figure 3 represents all species coexist around the interior equilibrium point $B_*^{(ii)}$ (43.4216, 21.0632, 6.6379) for $\sigma = 0.005$. The above results indicate that in the absence of cannibalism, all species coexist through an oscillatory manner. But it is interesting to note that all the species settle down to a stable position from the oscillatory behavior due to presence of cannibalism.

For $\sigma = 0.005$, the system (2.4) has two positive interior equilibrium points $B_*^{(i)}$ (15.1342, 20.5234, 6.3140) and $B_*^{(ii)}$ (43.4216, 21.0632, 6.6379). The eigenvalues of the system at $B_*^{(i)}$ are 0.180296 and $-0.0310664 \pm 0.0450505i$, so there exists a one-dimensional unstable manifold in x -axis and two-dimensional stable manifold in yz -plane. Therefore, the system is always unstable at $B_*^{(i)}$. On the other hand, the eigenvalues of another equilibrium point $B_*^{(ii)}$ are -0.179895 and $-0.0353087 \pm 0.0468876i$. Thus the system is always locally asymptotically stable around $B_*^{(ii)}$. In addition, Fig. 4 shows that the system is globally stable at the interior steady state $B_*^{(ii)}$ i.e., any trajectory starting from the positive region $E \in R_+^3$ (independent of initial conditions) converges to $B_*^{(ii)}$.

For $\sigma = 0.009017$ and the other parameters are same as in Table 2, the system (2.4) has two disease-free planar equilibrium points $B_2^{(i)}$ (0.2956, 1.9814, 0), $B_2^{(ii)}$ (29.1531, 30.6932, 0), and two interior equilibria $B_*^{(i)}$ (13.5781, 21.1779, 1.83203),

Table 2 List of variables and parameters

| Variable/Parameter | Biological meaning | Parameter value |
|--------------------|---|-----------------|
| x | Prey population size | – |
| y | Susceptible predator population size | – |
| z | Infected predator population size | – |
| r | Intrinsic per capita growth rate of prey | 0.4 |
| k | Carrying capacity of prey | 60.0 |
| α_1 | Predation rate of susceptible predator | 0.2 |
| α_2 | Predation rate of infected predator | 0.1 |
| γ | Half-saturation constant | 0.7 |
| α | Conversion efficiency of predator | 0.4 |
| λ | Disease transmission rate | 0.004 |
| d | Natural death rate of predator | 0.02 |
| e | Additional disease-related mortality rate | 0.01 |
| σ | Attack rate due to cannibalism | 0.005 |
| c_1 | Conversion rate of predator for cannibalism of susceptible predator | 0.3 |
| c_2 | Conversion rate of predator for cannibalism of infected predator | 0.2 |
| β | Dimensionless quantity ($0 < \beta < 1$) | 0.3 |
| l | Probability of transmission for cannibalistic interaction | 0.01 |
| f | Number of predator sharing one conspecific predator | 10.0 |

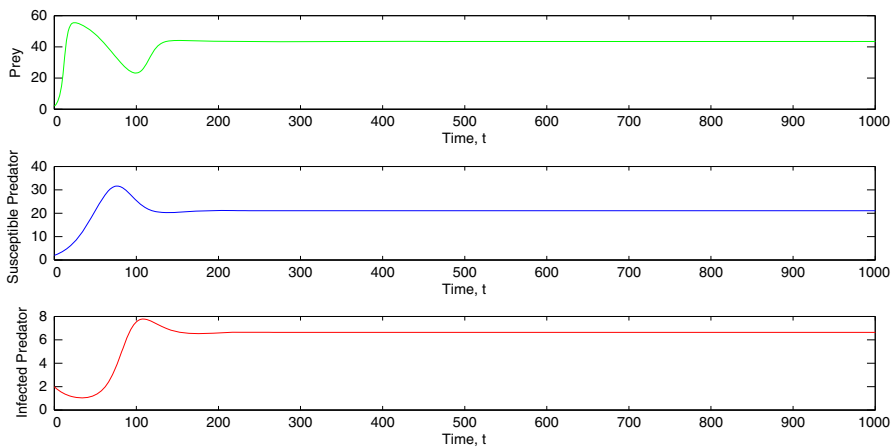


Fig. 3 Shows that all species coexist in stable position for $\sigma = 0.005$, $c_1 = 0.3$; $c_2 = 0.2$; $\beta = 0.3$; $l = 0.01$; $f = 10.0$ and other parameter values as in Fig. 2

$B_*^{(ii)}$ (44.9951, 21.8564, 1.99731). At the equilibrium point $B_2^{(i)}$, $\mu_1 = -0.025648$, $\mu_{2,3} = 0.056228 \pm 0.055224i$; similarly, at $B_2^{(ii)}$, $\mu_1 = 0.037420$, $\mu_2 = -0.051630$, $\mu_3 = -0.00003268$; and at $B_*^{(i)}$, $\mu_1 = 0.199053$, $\mu_{2,3} = -0.027732 \pm 0.024687i$. Thus the planar equilibria $B_2^{(i)}$ and $B_2^{(ii)}$ as well as one interior equilibrium point

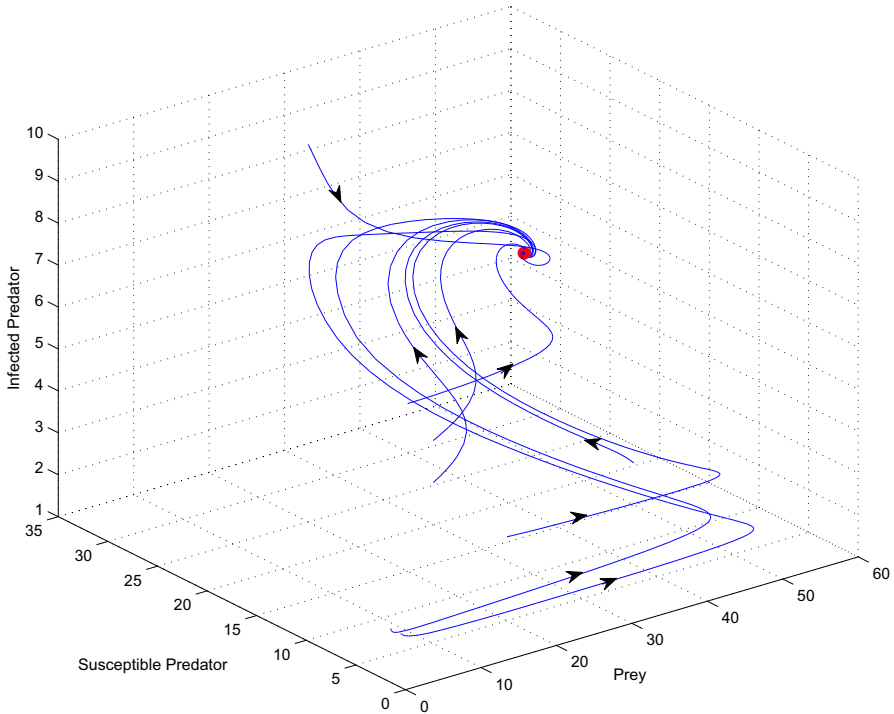


Fig. 4 Global stability of the system (2.4) around interior equilibrium point $B_*^{(ii)}$ (43.4216, 21.0632, 6.6379) for $\sigma = 0.005$ and other parameter values as in Table 2

$B_*^{(i)}$ of the system are always unstable around their corresponding equilibria, see Fig. 5. But only one interior equilibrium point $B_*^{(ii)}$ is locally asymptotically stable, since *Routh–Hurwitz criteria* $\Theta_1 = 0.264792 > 0$, $\Theta_3 = 0.000331857 > 0$ and $\Theta_1\Theta_2 - \Theta_3 = 0.00351124 > 0$ are satisfied at $B_*^{(ii)}$. Moreover, Fig. 5b shows that the interior equilibrium point $B_*^{(ii)}$ of the system is globally stable because Ω is positive definite. This means that the disease can invade in the system and go to the endemic levels.

Figure 6 demonstrates that the system will be disease free for $\sigma = 0.018$. By *Cardano’s method* the Eq. (4.1) has three distinct positive roots, so there are three different equilibrium points namely $B_2^{(i)}$ (0.3791, 2.1446, 0), $B_2^{(ii)}$ (7.2744, 14.0152, 0) and $B_2^{(iii)}$ (50.9464, 15.5862, 0). In this case among the three equilibrium points only one disease-free equilibrium point $B_2^{(iii)}$ is locally stable, since at $B_2^{(iii)}$ the disease basic reproduction number $R_{02} = 0.7918 < 1$, and $\sigma = 0.018 > \sigma^{[2]} = -0.0674$ and $r = 0.4 > r^{[2]} = 0.1402$. Thus the prey and susceptible predator population coexist in locally asymptotically stable position around the disease-free steady-state $B_2^{(iii)}$, which rule out the presence of disease. Moreover, the sufficient condition $r\gamma + (1 - c_1)\sigma\beta = 0.2838 \geq \alpha_1 = 0.2$ together with local stability conditions imply its global stability around $B_2^{(iii)}$. Figure 7a shows that the trajectories of the system (2.4) approach to the

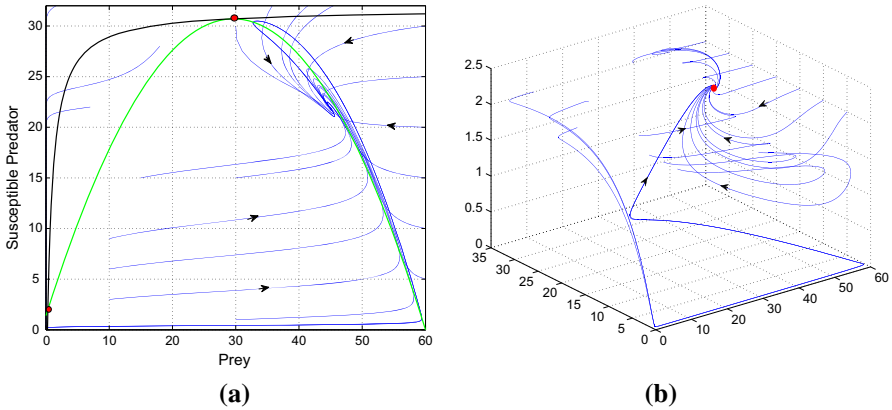


Fig. 5 The global dynamics of the system (2.4) for $\sigma = 0.009017$ and other parameter values as in Table 2. **a** Two planar equilibria $B_2^{(i)}$ (0.2956, 1.9814, 0) and $B_2^{(ii)}$ (29.1531, 30.6932, 0) of the model are unstable. **b** Interior equilibrium point $B_*^{(ii)}$ (44.9951, 21.8564, 1.99731) of the model is globally stable

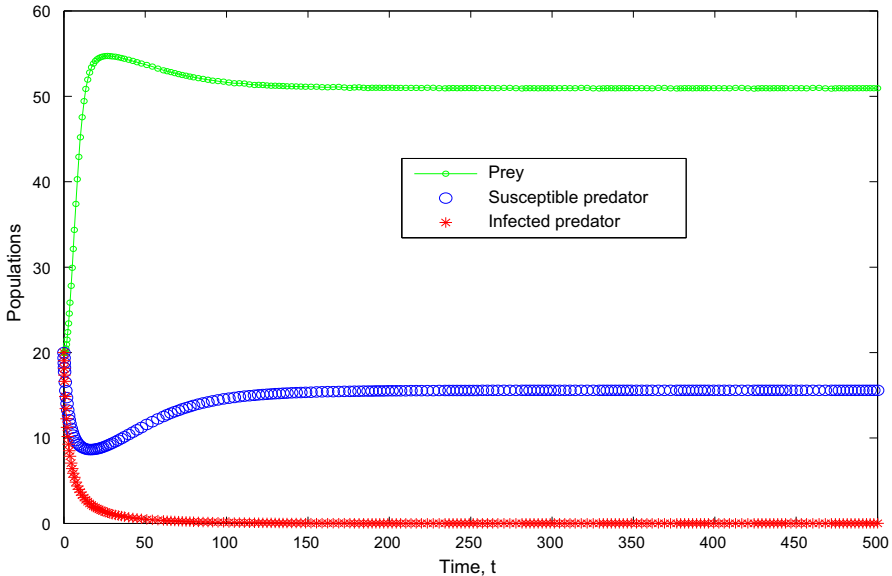


Fig. 6 Shows that extinction of infected predator in stable position for $\sigma = 0.018$ and other parameter values as in Fig. 2

steady-state $B_2^{(iii)}$ regardless of initial conditions. For $\sigma = 0.05$ the system (2.4) has only one disease-free planar equilibrium point $B_2(57.0811, 5.6219, 0)$ and is locally as well as globally stable around unique planar equilibrium point B_2 , see Fig. 7b.

Numerical simulation of the system (2.4) shows that all species coexist in limit cycle oscillation nature for $\sigma \leq 0.0026$. Disease-free system exhibits limit cycle oscillations in the range $0.0027 \leq \sigma \leq 0.0048$ and the system (2.4) shows a stable situation around the positive interior steady-state in the interval $0.0049 \leq \sigma < 0.013$.

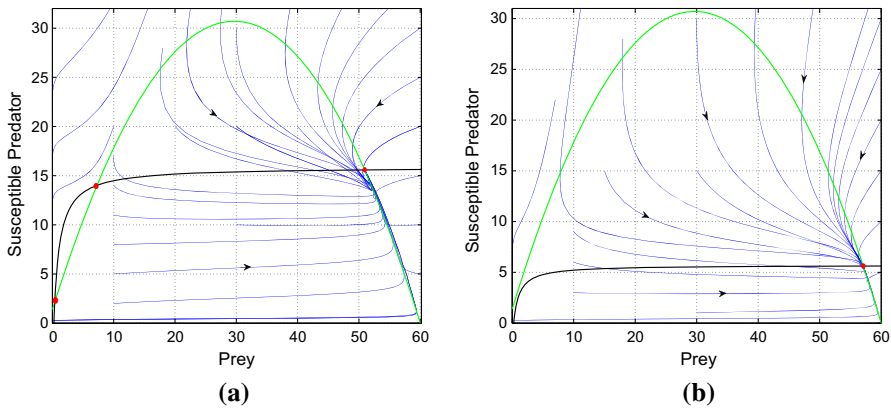


Fig. 7 The dynamics of the system (2.4) for **a** $\sigma = 0.018$, **b** $\sigma = 0.05$ and other parameter values as in Table 2. The *green line* represents x-nullcline and *black one* denotes the y-nullcline. **a** Global stability of the model around $B_2^{(iii)}$ (50.9464, 15.5862, 0) and the other equilibria $B_2^{(i)}$ (0.3791, 2.1446, 0) and $B_2^{(ii)}$ (7.2744, 14.0152, 0) are unstable. **b** Global stability of the model around unique planar equilibrium point B_2 (57.0811, 5.6219, 0). (Color figure online)

Finally, system (2.4) goes into the disease-free stable situation from the stable position around the interior equilibrium state for $\sigma > 0.013$. The bifurcation diagram (Fig. 8) w.r.t bifurcating parameter σ also reflects the above fact. It follows that there are three critical attack rate values so that (i) the unstable internal steady-state B_* switches to disease-free planar steady-state B_2 in an unstable situation (ii) comes back from unstable disease-free steady-state to interior steady-state in a stable position as σ increases, (iii) further increasing of cannibalistic attack rate σ , stable interior steady state switches to disease-free steady-state in stable position. Based on above numerical results, we get an interval $[0, 0.0026]$ where all species survive in limit cycle oscillation and for $\sigma \in [0.0027, 0.0048]$ disease goes into extinction, and prey and predator species survive in oscillatory behavior. Next, for $\sigma \in [0.0049, 0.013]$ all species survive in a stable position and for $\sigma > 0.013$ the disease is wipe out from the system. Thus, there exist three threshold values of σ which are denoted by σ_1^* ($=0.0026$), σ_2^* ($=0.0048$) and σ_3^* ($=0.013$). Our numerical experiments suggest that to control the disease propagation in predator population, a minimum threshold of cannibalistic attack rate σ_1^* ($=0.0026$) is required. *The disease-free predator-prey oscillations become stable when σ crosses a critical value σ_2^* ($=0.0048$).* Although, the disease is further spreads among the predator species. Thereafter, the disease cannot spread among the predators when σ passing through σ_3^* . This result indicates that there is a maximum threshold of cannibalistic attack rate σ_3^* ($=0.013$) above which the infected predator does not exist. *Therefore, cannibalism can prevent the population oscillation as well as disease in the system.*

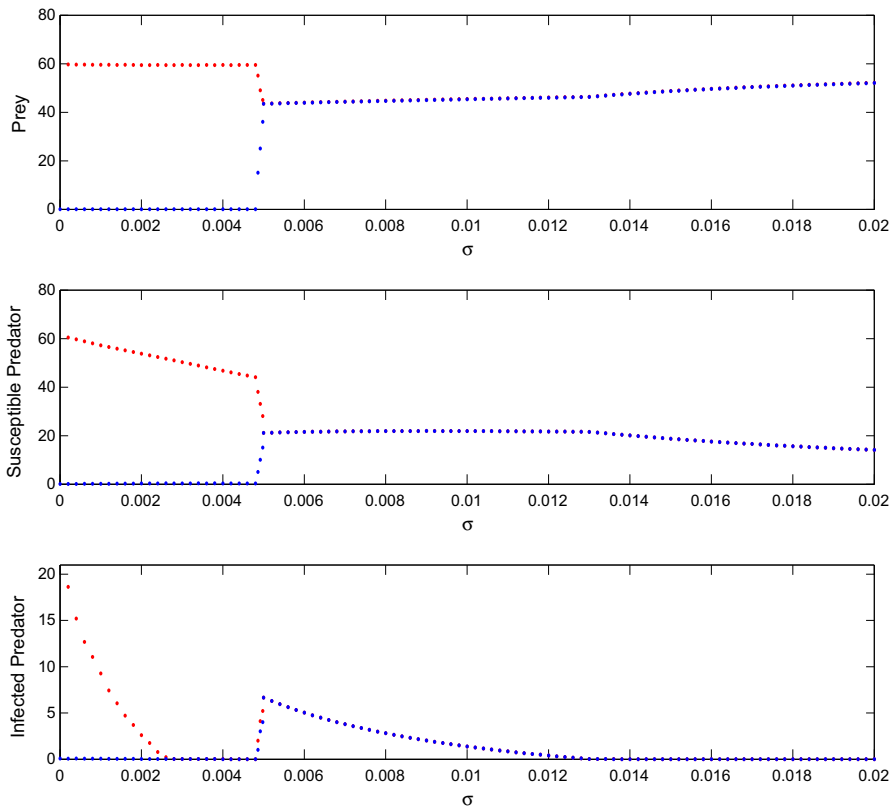


Fig. 8 Bifurcation diagram of system (2.4) for $\sigma \in [0.0, 0.02]$ and other parameter values as in Table 2

6.2 Dynamics of the system (2.4) for variation of both cannibalistic conversion rates c_1, c_2

Now we are interested to observe the effects of conversion rates c_1 and c_2 in the system (2.4). To do this, we first vary the parameter c_1 , keeping c_2 and other parameter values fixed. Next, we vary c_2 , keeping c_1 and other parameter values fixed as in the Table 2. In some situation, conversion rates due to cannibalism help the coexistence of all species or disease eradicated from the predator species. We observed that for a certain range of conversion rate c_1 , the infected predator population extinct. All species coexist in a stable position for $c_1 \in [0, 0.3]$. It is observed that infected predator goes to extinction as well as disease-free predator and prey population exist in oscillatory nature in the range $(0.3, 0.9)$. Clearly, the situation represents the dynamics of a disease-free system. Further, if we increase the value of c_1 from 0.9, the disease is again spreading among the predators, and all species coexist in a limit cycle nature. For clear dynamics, we draw a bifurcation diagram (Fig. 9) for different values of c_1 .

Figure 10 indicates a situation where the infected predator survives in a stable steady-state for $c_2 \in [0, 0.265]$. Also the infected predator increases as increasing

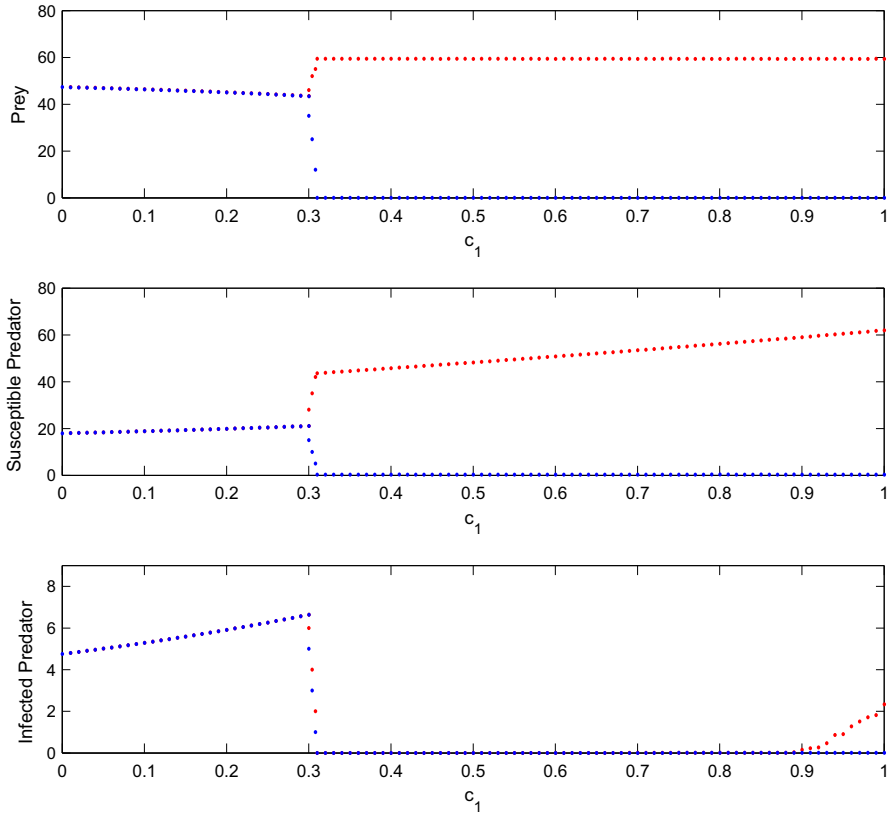


Fig. 9 Bifurcation diagram of system (2.4) for $c_1 \in (0.0, 1.0)$ and other parameter values as in Table 2

with c_2 in the range $0 \leq c_2 \leq 0.265$ and goes to its maximum value at $c_2 \approx 0.265$. When c_2 cross a critical value $c_2^0 (=0.265)$, the disease wipes out from the system and disease-free predator, and prey population exists in limit cycle oscillation. In this case, a minimum conversion efficiency c_2^0 is required to control the disease propagation among the predators. Thus we conclude that all species will be disease free for higher values of conversion rates c_1 (but not exceeding 0.9) and c_2 .

6.3 Effect of disease transmission rate λ in the system (2.4)

From a biological point of view, the disease in predator population also plays an important role. We observe the effect of disease in the system (2.4) for the variation of force of infection λ , keeping the other parameters are fixed as in Table 2. For $\lambda < 0.004$ the system shows limit cycle oscillation dynamics in a prey and disease-free predator populations (Fig. 11a). All species coexist around $B_*^{(ii)}$ (43.4216, 21.0632, 6.6379) and the system enters into the steady-stable position from limit cycle oscillation for $\lambda = 0.004$ (see Fig. 11b). In this situation, the disease basic reproduction number

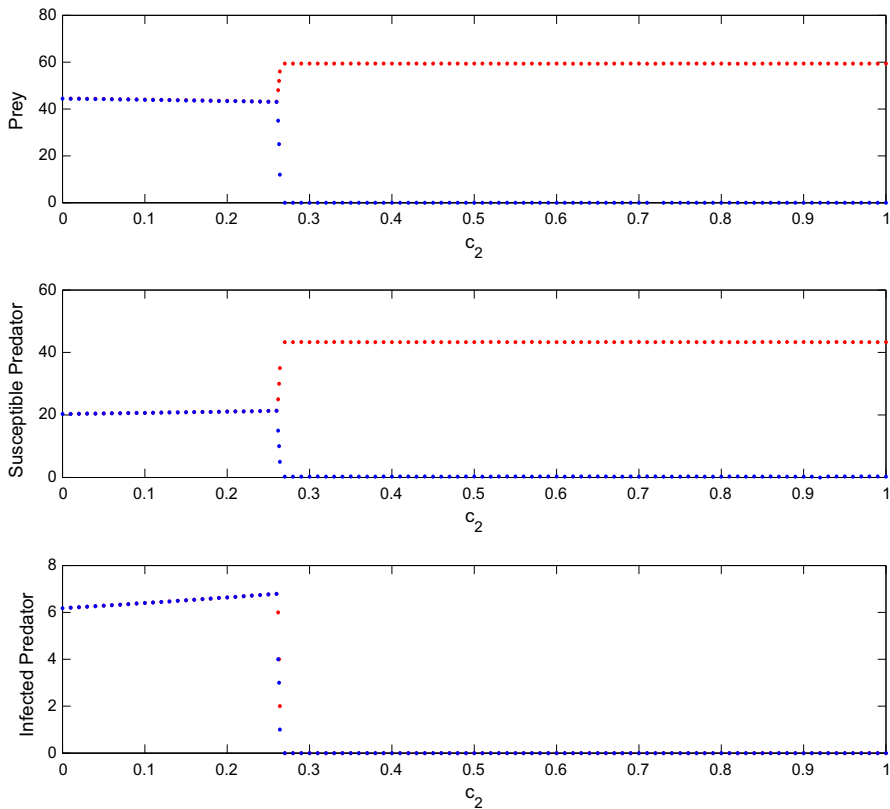


Fig. 10 Bifurcation diagram of system (2.4) for $c_2 \in (0.0, 1.0)$ and other parameter values as in Table 2

at $B_*^{(ii)}$ is $R_{02} = 1.53884 > 1$, so the disease spreads among the predators. Thus a minimum strength of infection ($\lambda_{min} = 0.004$) is required for propagation of disease in the predator population or stabilize the oscillatory existence of disease-free system into stable coexistence of all species. From above numerical result, we get an interval $[0, 0.004)$ on λ in which disease-free prey–predator species exist in oscillatory behavior. To make it clearer, we plot a bifurcation diagram of all species for variation of infection rate λ , see Fig. 12. It is observed from Fig. 12 susceptible predator decrease as increasing with λ but the infection cannot invade among the whole predator population. We finally conclude that there is a critical value of disease transmission rate (λ_{min}), so that the disease-free planar steady-state B_2 switches from unstable to stable interior steady state B_* .

6.4 Role of different conversion efficiency α of predator

Now we observe the effects on the system (2.4) for changing the conversion efficiency α in the predator species. The Fig. 13 indicates that predator-free prey only steady-state exists in a stable position at a positive level for $\alpha \in [0, 0.1]$, disease-

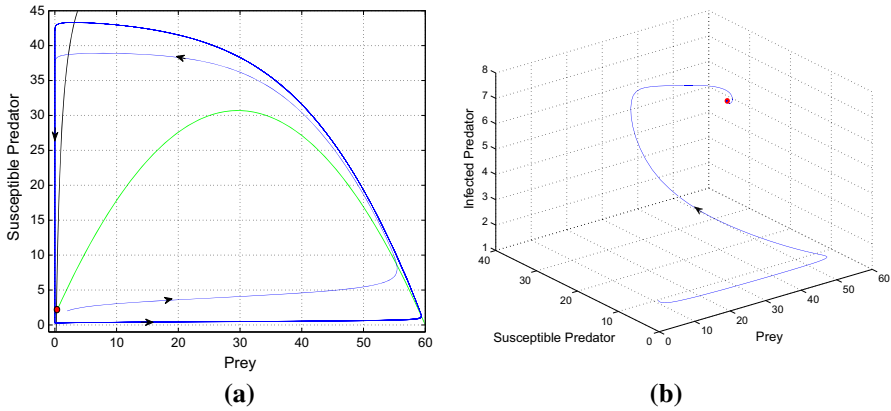


Fig. 11 The dynamics of the system (2.4) for $\mathbf{a} \lambda = 0.003$, $\mathbf{b} \lambda = 0.004$ and other parameter values as in Table 2. **a** Oscillatory behavior of the system around $B_2(0.2658, 1.9231, 0)$. **b** Stability of the system around interior equilibrium point $B_*^{(ii)}(43.4216, 21.0632, 6.6379)$

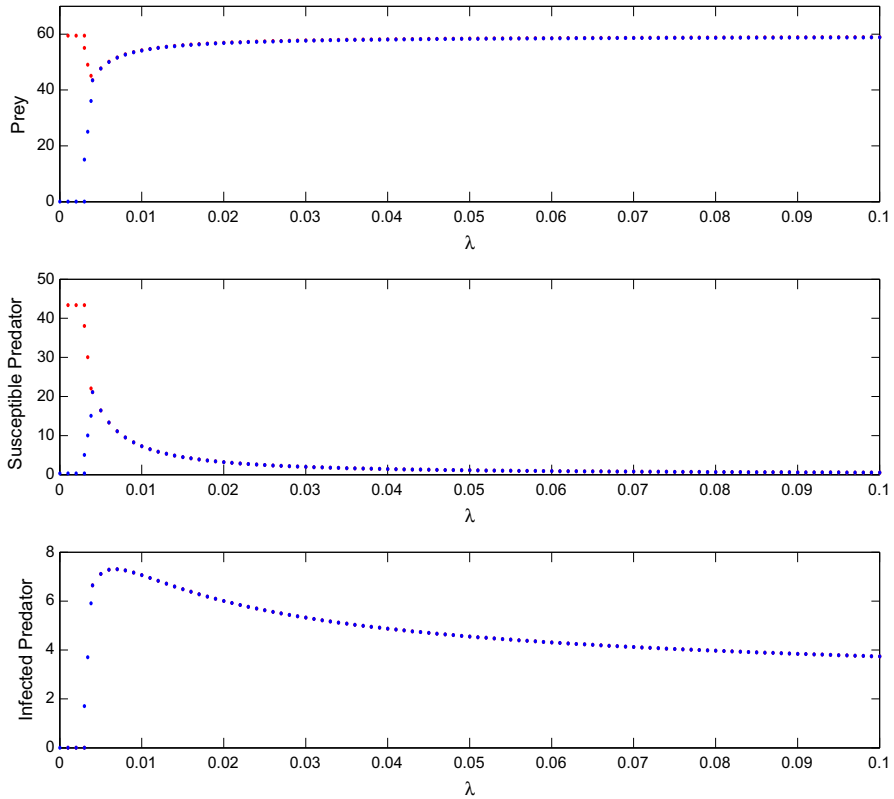


Fig. 12 Bifurcation diagram of system (2.4) for $\lambda \in [0.0, 0.1]$ and other parameter values as in Table 2

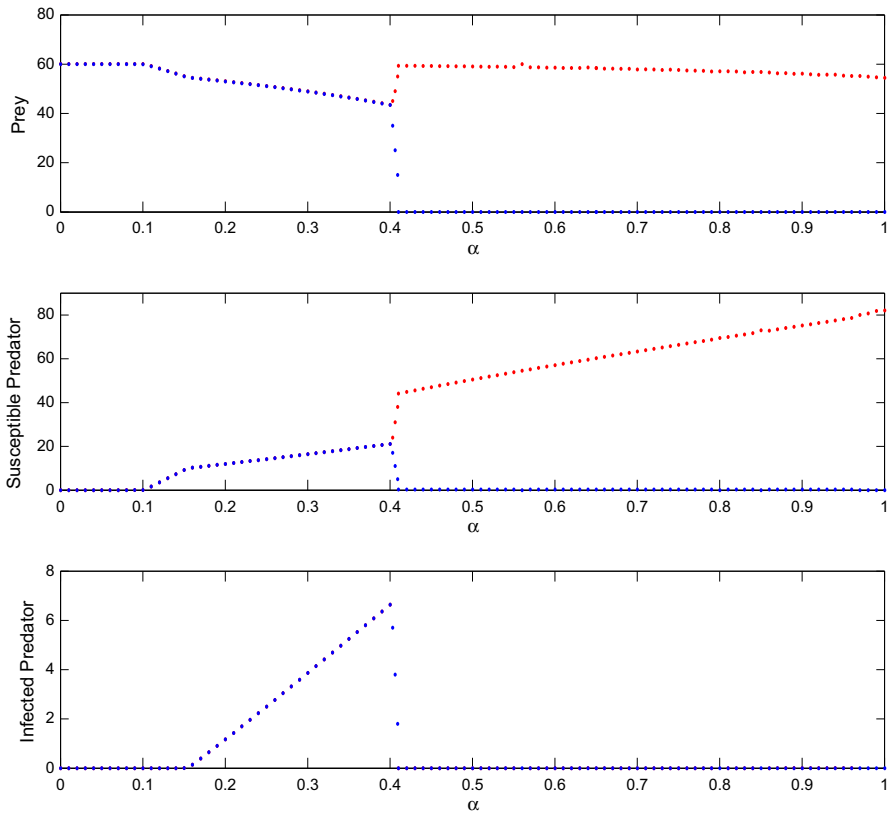


Fig. 13 Bifurcation diagram of system (2.4) for $\alpha \in (0.0, 1.0)$ and other parameter values as in Table 2

free predator and prey populations coexist in a stable position at a positive level for $\alpha \in (0.1, 0.15)$. Further, it is observed that all species coexist in a stable position around the interior steady-state for $\alpha \in [0.15, 0.4]$. *It is worthy to note here that the system (2.4) undergoes a transcritical bifurcation between predator-free equilibrium point (B_1) and disease-free equilibrium point (B_2) at $\alpha = 0.1$. We also observe that at $\alpha = 0.15$ the system (2.4) undergoes a transcritical bifurcation between disease-free equilibrium point (B_2) and the interior equilibrium point (B_*).* Again, increasing the value of $\alpha (>0.4)$ implies that the prey and susceptible predator population exist in limit cycle oscillation. Thus we can get an important result that the higher value of the conversion efficiency α , control the spreads of disease in the predator population and can give rise a bifurcating periodic solution around disease-free equilibrium point. So there is a maximum threshold of the conversion rate α ($\alpha_{max} = 0.4$) above which the infected predator doesn't survive in the system.

For better visualization of the stability dynamics of the system (2.4), we draw the stability region of the equilibrium points B_1 , B_2 and B_* . We draw the stability region of the system (2.4) in $\sigma - \lambda$ parameter space (Fig. 14). In Fig. 14, the blue shaded region (R_2) indicates the stability region of the disease-free equilibrium (B_2), the red

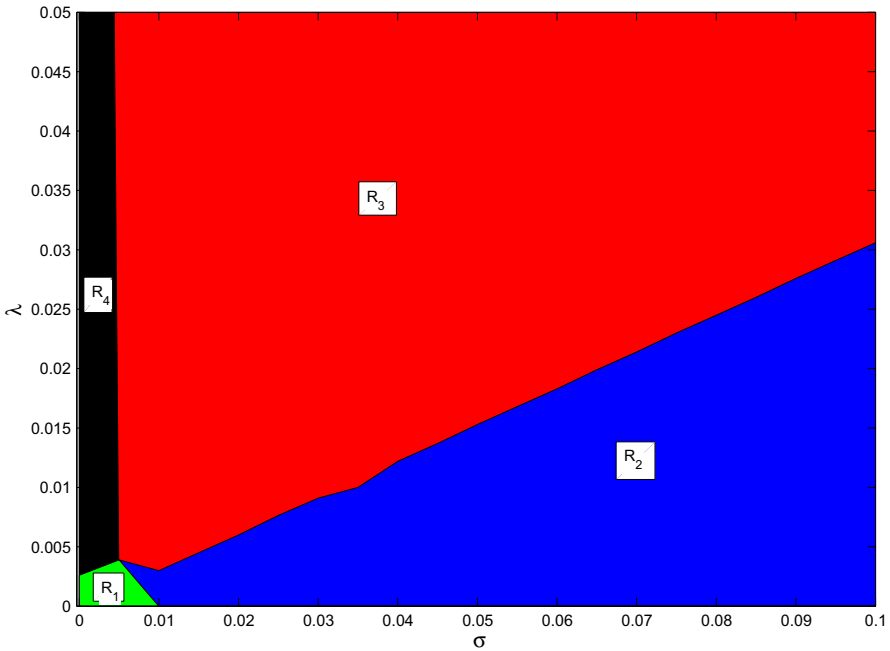


Fig. 14 Domains of stability and instability of the system (2.4) in σ - λ parameter space where other parameter values are taken from Table 2. The horizontal axis represents the cannibalistic attack rate σ and the vertical axis represents the disease transmission coefficient λ . The green region (R_1) depicts that the disease-free equilibrium point B_2 is oscillation in nature; the blue region (R_2) depicts that the disease-free equilibrium B_2 is stable; the red region (R_3) indicates the stability region of the interior equilibrium point B_* ; on the other hand, The black region (R_4) depicts that the interior equilibrium point B_* is oscillation in nature. (Color figure online)

region (R_3) indicates the stability region of the interior equilibrium B_* , the black region (R_4) indicates the limit cycle oscillation region of the interior equilibrium B_* , and the green region (R_1) indicates the limit cycle oscillation region around the disease-free equilibrium point (B_2).

We observe that for any value of λ (<0.0039), if the cannibalistic attack rate σ is above (or below) a threshold value, then the system becomes disease free (or limit cycle oscillatory nature around the disease-free equilibrium point B_2). We also observe that for the small value of σ (<0.005), if the force of infection λ is greater than a threshold value, then the system becomes oscillatory nature around the interior equilibrium B_* . For the moderate value of cannibalistic attack rate σ , all species coexist in a stable nature. Now if the value of cannibalistic attack rate is high enough, i.e. cannibalistic attack together with disease induced extra mortality reduces the infection in predator, then the system becomes disease free.

We have drawn the stability region of the system (2.4) in $\sigma - \alpha$ parameter space. In Fig. 15, green (R_1), blue (R_2), red (R_3) and yellow (R_4) shaded regions indicate the oscillation of the disease-free (B_2), stability of disease-free (B_2), stability of the interior equilibrium point (B_*) and the stability of prey only equilibrium point (B_1),

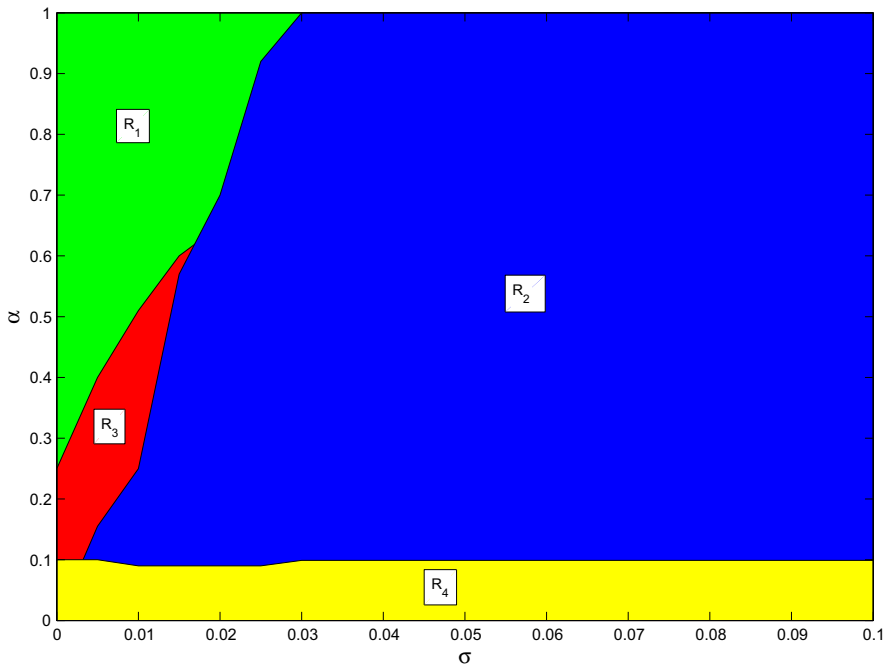


Fig. 15 Domains of stability and instability of the system (2.4) in σ - α parameter space where other parameter values are taken from Table 2. The horizontal axis represents the cannibalistic attack rate σ and the vertical axis represents the conversion efficiency α . The green region (R_1) depicts that the disease-free equilibrium point B_2 is oscillation in nature; the blue region (R_2) depicts that the disease-free equilibrium B_2 is stable; the red region (R_3) indicates the stability region of the interior equilibrium point B_* ; on the other hand, the yellow region (R_4) indicates the stability region of prey only equilibrium point B_1 . (Color figure online)

respectively. We observe that for any value of σ , if the conversion efficiency (α) of predator is less than a threshold value, then the system becomes predator free (B_1). For the moderate value of conversion efficiency, then all species coexist in the system when the attack rate σ is low. Now if the value of σ is high enough, the system becomes disease free. Disease-free equilibrium point (B_2) is oscillatory nature when α is high enough and the value of σ is moderate. Further, if we increase the cannibalistic attack rate σ , then the disease-free equilibrium point (B_2) becomes stable.

We have also drawn the stability region of the system (2.4) in λ - α parameter space. In Fig. 16, black (R_1), blue (R_2), red (R_3) and yellow (R_4) shaded regions indicate the oscillation of interior equilibrium point (B_*), stability of disease-free (B_2), stability of the interior equilibrium point (B_*) and the stability of predator-free equilibrium point (B_1), respectively. We observe that for any value of λ , if α is less than a threshold value, then the system becomes predator-free (B_1). For the moderate value of α , the system becomes *disease-free* (B_2) when the value of force of infection λ is moderate. We also observe that for the value of α is greater than a threshold value, then the system becomes oscillatory nature around the interior equilibrium B_* when λ is small. Now if the value of force of infection λ is high enough, then all the species coexist in the system.

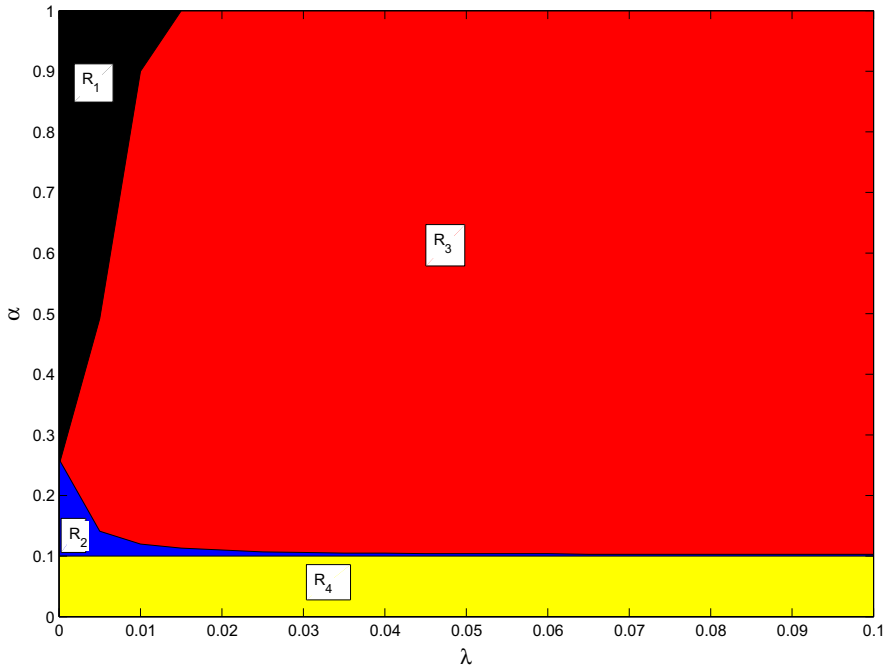


Fig. 16 Domains of stability and instability of the system (2.4) in λ - α parameter space where other parameter values are taken from Table 2. The *horizontal* axis represents the disease transmission coefficient λ and the *vertical* axis represents the conversion efficiency α . The *black* region (R_1) depicts that the interior equilibrium point B_* is oscillation in nature; the *blue* region (R_2) depicts that the disease-free equilibrium B_2 is stable; the *red* region (R_3) indicates the stability region of the interior equilibrium point B_* ; on the other hand, the *yellow* region (R_4) indicates the stability region of prey only equilibrium point B_1 . (Color figure online)

7 Conclusion

In this article, we proposed and analyzed a cannibalistic eco-epidemiological model with disease in the predator population. The characteristic behavior of the predator species follows Holling type II functional response. In the presence of disease, the predator community is subdivided into two classes viz. susceptible and infected. The susceptible predator becomes infected through contact with infected predator and/or disease spreading among predators during the process of cannibalistic interaction with infected predator. We have considered that the contact rate between the infected and susceptible predator obeys the law of mass action. The main objective of this work is to study the effects of cannibalistic attack rate (σ), cannibalistic conversion rates (c_1, c_1), force of infection (λ), and conversion efficiency (α) of predators in the system dynamics. We have identified and analyzed the different equilibrium points of the model for ecological importance: (i) axial steady state consisting only of the prey species (ii) the boundary disease-free steady state, and (iii) the coexistence steady state. The preliminary results like existence, positivity and boundedness of solutions, and extinction criterion of the species of the model (2.4) are prescribed in Sect. 3. We

have analyzed the disease-free boundary steady state from local as well as global perspective. We have obtained disease basic reproduction number R_{02} , threshold values $\sigma^{[2]}$ of cannibalistic attack rate and $r^{[2]}$ of prey's intrinsic growth rate such that for $R_{02} < 1$, $\sigma > \sigma^{[2]}$ and $r > r^{[2]}$, the system become locally disease-free stable characteristic. These results imply, a higher cannibalistic attack rate is required to eradicate the disease from the system because R_{02} and $r^{[2]}$ are decreasing as increases with σ . So cannibalism pressure plays a crucial role to prevent the spread of the disease infection among the predators. In addition, the system becomes the globally stable characteristic of the disease-free region in xy -plane if it is locally stable with additional sufficient condition $r\gamma + (1 - c_1)\sigma\beta \geq \alpha_1$ is required. Thus cannibalism has important consequences for control of disease transmission and/ extinction of infection in the host population.

Investigation of local as well as global stability of the model around the interior steady state showed that the system will exhibit local asymptotic stability around B_* if the conditions stated in the Theorem 3(a) hold. We study the global nature using Lyapunov functions. To visualize the role of key parameter cannibalism pressure (σ) for local as well as global perspective, we provide a comparison Table 1. Next, we have investigated the bifurcation dynamics around the endemic steady state. The Hopf-bifurcation diagrams with respect to key parameters σ , c_1 , c_1 , λ and α are drawn. Stability switching of prey and predator species is clear from bifurcation diagrams (see Figs. 8, 9, 10, 12, 13). Finally, applying the Butler–McGehee lemma, we find the conditions for the permanence of the system.

Our numerical observations suggest that the disease will spread among the predators when the force of infection (λ) in predator species is above some threshold value. Also, it has been observed that low rate of cannibalistic attack rate is needed for coexistence of prey and predator population in oscillatory nature. Although, when the cannibalistic attack rate (σ) is above a critical value, the oscillation in the populations disappears; stability switching occurs and the system becomes stable. This result disagrees with the result: cannibalism act as a destabilizing force in a predator–prey system studied by Magnússon [40]. Many species (see [21,44]) showed stabilizing effect of cannibalism on population dynamics. Therefore, cannibalism enhances the stability of the population dynamics as the increase in cannibalistic attack implies an increase of predator mortality, which decreases predator population size and the predation pressure on prey population. This leads to increase prey species size. Thus cannibalism can act as a mechanism that provides the necessary mortality to stabilize a host population during the adverse environmental conditions. Further, when the cannibalistic *attack rate is high enough* the system becomes disease-free. Therefore, it follows that the cannibalism pressure in the predator population is crucial for disease eradication and controlling the oscillation of the populations.

Acknowledgements The authors are grateful to the anonymous reviewers for their careful reading and valuable comments on the previous version of the paper which help us a lot to improve the manuscript. The research work of Sudip Samanta is supported by NBHM postdoctoral fellowship. Santosh Biswas's research work is supported by DST-PURSE project (Phase II).

Appendix 1

(a) The Jacobian matrix around the interior equilibrium point $B_*(x_*, y_*, z_*)$ is given by

$$J^* = \begin{bmatrix} V_{11} & V_{12} & V_{13} \\ V_{21} & V_{22} & V_{23} \\ V_{31} & V_{32} & V_{33} \end{bmatrix},$$

where $V_{11} = -\frac{rx_*}{k} + \frac{(\alpha_1 y_* + \alpha_2 z_*)x_*}{(\gamma + x_*)^2}$, $V_{12} = -\frac{\alpha_1 x_*}{\gamma + x_*}$, $V_{13} = -\frac{\alpha_2 x_*}{\gamma + x_*}$, $V_{21} = \frac{\alpha(\alpha_1 y_* + \alpha_2 z_*)}{\gamma + x_*} - \frac{\alpha(\alpha_1 y_* + \alpha_2 z_*)x_*}{(\gamma + x_*)^2}$, $V_{22} = \frac{\alpha\alpha_1 x_*}{\gamma + x_*} + c_1\sigma(2\beta y_* + z_*) + c_2\sigma\beta z_* - \sigma(2\beta y_* + z_*) - \sigma l f z_* - \lambda z_* - d$, $V_{23} = \frac{\alpha\alpha_2 x_*}{\gamma + x_*} + c_1\sigma y_* + c_2\sigma(\beta y_* + 2z_*) - \sigma y_* - \sigma l f y_* - \lambda y_*$, $V_{31} = 0$, $V_{32} = \lambda z_* + \sigma l f z_* - \sigma\beta z_*$, $V_{33} = -\sigma z_*$. The characteristic equation for J^* is

$$\mu^3 + \Theta_1\mu^2 + \Theta_2\mu + \Theta_3 = 0, \tag{7.1}$$

where $\Theta_1 = -(V_{11} + V_{22} + V_{33})$, $\Theta_2 = V_{11}V_{22} + V_{11}V_{33} + V_{22}V_{33} - V_{12}V_{21} - V_{23}V_{32}$, $\Theta_3 = -\det(J^*) = V_{11}V_{23}V_{32} + V_{12}V_{21}V_{33} - V_{13}V_{21}V_{32} - V_{11}V_{22}V_{33}$. According to the *Routh–Hurwitz* criteria the interior equilibrium point B_* is stable if the conditions stated in the theorem hold.

(b) Let Σ be a positive definite *Lyapunov* function about $B_*(x_*, y_*, z_*)$, given by

$$\Sigma = \Sigma_x + \Sigma_y + \Sigma_z,$$

where $\Sigma_x = x - x_* - x_* \ln \frac{x}{x_*}$, $\Sigma_y = y - y_* - y_* \ln \frac{y}{y_*}$, $\Sigma_z = z - z_* - z_* \ln \frac{z}{z_*}$. Now, computing the time derivative of Σ_x along the solution of (2.4), we obtain

$$\begin{aligned} \dot{\Sigma}_x &= (x - x_*) \left[r \left(1 - \frac{x}{k} \right) - \frac{\alpha_1 y + \alpha_2 z}{\gamma + x} \right] \\ &= (x - x_*) \left[-\frac{r(x - x_*)}{k} \right] - \alpha_1 \left(\frac{y}{\gamma + x} - \frac{y_*}{\gamma + x_*} \right) - \alpha_2 \left(\frac{z}{\gamma + x} - \frac{z_*}{\gamma + x_*} \right) \\ &= -\frac{r}{k}(x - x_*)^2 - \frac{\alpha_1}{(\gamma + x)}(x - x_*)(y - y_*) - \frac{\alpha_2}{(\gamma + x)}(x - x_*)(z - z_*) \\ &\quad + \frac{(\alpha_1 y_* + \alpha_2 z_*)}{(\gamma + x)(\gamma + x_*)}(x - x_*)^2. \end{aligned}$$

Similarly,

$$\begin{aligned} \dot{\Sigma}_y &= (y - y_*) \left[\frac{\alpha(\alpha_1 y + \alpha_2 z)x}{(\gamma + x)y} + c_1\sigma(\beta y + z) \right. \\ &\quad \left. + c_2\sigma \left(\beta + \frac{z}{y} \right) z - \sigma(\beta y + z) - \sigma l f z - \lambda z - d \right] \end{aligned}$$

$$\begin{aligned}
&= (y - y_*) \left[\alpha\alpha_1 \left(\frac{x}{\gamma + x} - \frac{x_*}{\gamma + x_*} \right) + \alpha\alpha_2 \left\{ \frac{xz}{(\gamma + x)y} - \frac{x_*z_*}{(\gamma + x_*)y_*} \right\} \right. \\
&\quad \left. - \sigma(1 - c_1)\beta(y - y_*) - \{\sigma(1 - c_1) - c_2\sigma\beta + \sigma lf + \lambda\}(z - z_*) \right. \\
&\quad \left. + c_2\sigma \left(\frac{z^2}{y} - \frac{z_*^2}{y_*} \right) \right] \\
&= \left\{ \frac{\alpha\alpha_1\gamma}{(\gamma + x)(\gamma + x_*)} + \frac{\alpha\alpha_2\gamma z_*}{(\gamma + x)(\gamma + x_*)y} \right\} (x - x_*)(y - y_*) \\
&\quad + \left[c_2\sigma \frac{z}{y} + c_2\sigma \frac{z_*}{y} - \{\sigma(1 - c_1) - c_2\sigma\beta + \sigma lf + \lambda\} \right. \\
&\quad \left. + \frac{\alpha\alpha_2x}{(\gamma + x)y} \right] (y - y_*)(z - z_*) \\
&\quad - \left\{ \sigma(1 - c_1)\beta + \frac{c_2\sigma z_*^2}{y_*y} + \frac{\alpha\alpha_2x_*z_*}{(\gamma + x_*)y_*y} \right\} (y - y_*)^2, \\
\dot{\Sigma}_z &= (z - z_*)[\lambda y + \sigma lf y - \sigma(\beta y + z) - (d + e)] \\
&= (\lambda + \sigma lf - \sigma\beta)(y - y_*)(z - z_*) - \sigma(z - z_*)^2.
\end{aligned}$$

Adding these quantities and after some algebraic calculations, we can obtain

$$\begin{aligned}
\dot{\Sigma} &= - \left[\left\{ \frac{r}{k} - \frac{(\alpha_1 y_* + \alpha_2 z_*)}{(\gamma + x)(\gamma + x_*)} \right\} (x - x_*)^2 \right. \\
&\quad + \left\{ \sigma(1 - c_1)\beta + \frac{c_2\sigma z_*^2}{y_*y} + \frac{\alpha\alpha_2x_*z_*}{(\gamma + x_*)y_*y} \right\} (y - y_*)^2 + \sigma(z - z_*)^2 \\
&\quad + \left\{ \frac{\alpha_1}{(\gamma + x)} - \frac{\alpha\alpha_1\gamma}{(\gamma + x)(\gamma + x_*)} - \frac{\alpha\alpha_2\gamma z_*}{(\gamma + x)(\gamma + x_*)y} \right\} \\
&\quad \times (x - x_*)(y - y_*) \\
&\quad + \left\{ \sigma(1 - c_1) + \sigma\beta(1 - c_2) - c_2\sigma \frac{z}{y} - c_2\sigma \frac{z_*}{y} - \frac{\alpha\alpha_2x}{(\gamma + x)y} \right\} (y - y_*)(z - z_*) \\
&\quad \left. + \frac{\alpha_2}{(\gamma + x)} (x - x_*)(z - z_*) \right]
\end{aligned}$$

The above expression can be written in the form $-\mathbf{w}^T \Omega \mathbf{w}$, where $\mathbf{w} = (x - x_*, y - y_*, z - z_*)$ and Ω is the symmetric matrix given by

$$\Omega = \begin{pmatrix} \Omega_{11} & \Omega_{12} & \Omega_{13} \\ \Omega_{12} & \Omega_{22} & \Omega_{23} \\ \Omega_{13} & \Omega_{23} & \Omega_{33} \end{pmatrix},$$

with $\Omega_{11} = \frac{r}{k} - \frac{(\alpha_1 y_* + \alpha_2 z_*)}{(\gamma+x)(\gamma+x_*)}$, $\Omega_{12} = \frac{1}{2} \left\{ \frac{\alpha_1}{(\gamma+x)} - \frac{\alpha\alpha_1\gamma}{(\gamma+x)(\gamma+x_*)} - \frac{\alpha\alpha_2\gamma z_*}{(\gamma+x)(\gamma+x_*)y} \right\}$, $\Omega_{13} = \frac{1}{2} \frac{\alpha_2}{(\gamma+x)}$, $\Omega_{22} = \sigma(1-c_1)\beta + \frac{c_2\sigma z_*^2}{y_*y} + \frac{\alpha\alpha_2 x_* z_*}{(\gamma+x_*)y_*y}$, $\Omega_{23} = \frac{1}{2} \{ \sigma(1-c_1) + \sigma\beta(1-c_2) - c_2\sigma \frac{z_*}{y} - c_2\sigma \frac{z_*}{y} - \frac{\alpha\alpha_2 x_*}{(\gamma+x)y} \}$, $\Omega_{33} = \sigma$.

Thus, Σ is negative definite if the symmetric matrix Ω is positive definite. The matrix Ω is positive definite, if all the principal minors $\mathbb{P}_1 = \Omega_{11}$, $\mathbb{P}_2 = \Omega_{11}\Omega_{22} - \Omega_{12}^2$, $\mathbb{P}_3 = \Omega_{11}\Omega_{22}\Omega_{33} + 2\Omega_{12}\Omega_{13}\Omega_{23} - \Omega_{11}\Omega_{23}^2 - \Omega_{22}\Omega_{13}^2 - \Omega_{33}\Omega_{12}^2$ of Ω are positive, i.e.,

- (i) $\mathbb{P}_1 = \frac{r}{k} - \frac{(\alpha_1 y_* + \alpha_2 z_*)}{(\gamma+x)(\gamma+x_*)} > 0$,
- (ii) $\mathbb{P}_2 = \left[\frac{r}{k} - \frac{(\alpha_1 y_* + \alpha_2 z_*)}{(\gamma+x)(\gamma+x_*)} \right] \left[\sigma(1-c_1)\beta + \frac{c_2\sigma z_*^2}{y_*y} + \frac{\alpha\alpha_2 x_* z_*}{(\gamma+x_*)y_*y} \right] - \left[\frac{1}{2} \left\{ \frac{\alpha_1}{(\gamma+x)} - \frac{\alpha\alpha_1\gamma}{(\gamma+x)(\gamma+x_*)} - \frac{\alpha\alpha_2\gamma z_*}{(\gamma+x)(\gamma+x_*)y} \right\} \right]^2 > 0$,
- (iii) $\mathbb{P}_3 = \Omega_{33}(\Omega_{11}\Omega_{22} - \Omega_{12}^2) + \Omega_{23}(\Omega_{12}\Omega_{13} - \Omega_{11}\Omega_{23}) + \Omega_{13}(\Omega_{12}\Omega_{23} - \Omega_{22}\Omega_{13}) > 0$.

For \mathbb{P}_1 , we have by (4.3) $\mathbb{P}_1(x) = \frac{r}{k} - \frac{(\alpha_1 y_* + \alpha_2 z_*)}{(\gamma+x)(\gamma+x_*)} > \mathbb{P}_1(0) = \frac{r}{k} - \frac{(\alpha_1 y_* + \alpha_2 z_*)}{\gamma(\gamma+x_*)} > 0$ since $\mathbb{P}_1(x) = \frac{(\alpha_1 y_* + \alpha_2 z_*)}{(\gamma+x)^2(\gamma+x_*)} > 0$.

For \mathbb{P}_2 , using (4.3) and (4.4), we have

$$\begin{aligned} \mathbb{P}_2 &= \left[\frac{r}{k} - \frac{\alpha_1 y_* + \alpha_2 z_*}{(\gamma+x)(\gamma+x_*)} \right] \left[\sigma(1-c_1)\beta + \frac{c_2\sigma z_*^2}{y_*y} + \frac{\alpha\alpha_2 x_* z_*}{(\gamma+x_*)y_*y} \right] \\ &\quad - \left[\frac{1}{2} \left\{ \frac{\alpha_1}{(\gamma+x)} - \frac{\alpha\alpha_1\gamma}{(\gamma+x)(\gamma+x_*)} - \frac{\alpha\alpha_2\gamma z_*}{(\gamma+x)(\gamma+x_*)y} \right\} \right]^2 \\ &= \left[\left\{ \left(\frac{r}{k} - \frac{\alpha_1 y_* + \alpha_2 z_*}{(\gamma+x)(\gamma+x_*)} \right) \sigma(1-c_1)\beta - \frac{1}{4} \left(\frac{\alpha_1}{\gamma+x} \right)^2 \right\} \right. \\ &\quad \left. + \left\{ \frac{r}{k} - \frac{\alpha_1 y_* + \alpha_2 z_*}{(\gamma+x)(\gamma+x_*)} \right\} \left\{ \frac{c_2\sigma z_*^2}{y_*y} + \frac{\alpha\alpha_2 x_* z_*}{(\gamma+x_*)y_*y} \right\} \right. \\ &\quad \left. + \frac{1}{2} \frac{\alpha\alpha_1\alpha_2\gamma z_*}{(\gamma+x)^2(\gamma+x_*)y} \left(1 - \frac{\alpha\gamma}{\gamma+x_*} \right) + \frac{1}{4} \frac{\alpha\alpha_1^2\gamma}{(\gamma+x)^2(\gamma+x_*)} \left(1 - \frac{\alpha\gamma}{\gamma+x_*} \right) \right. \\ &\quad \left. + \frac{1}{4} \frac{\alpha\gamma}{(\gamma+x)^2(\gamma+x_*)} \left\{ \alpha_1^2 - \frac{\alpha\alpha_2^2\gamma z_*^2}{(\gamma+x_*)y^2} \right\} \right] \\ &> \left[\left\{ \left(\frac{r}{k} - \frac{\alpha_1 y_* + \alpha_2 z_*}{\gamma(\gamma+x_*)} \right) \sigma(1-c_1)\beta \right. \right. \\ &\quad \left. \left. - \frac{1}{4} \left(\frac{\alpha_1}{\gamma} \right)^2 \right\} + \left\{ \frac{r}{k} - \frac{\alpha_1 y_* + \alpha_2 z_*}{\gamma(\gamma+x_*)} \right\} \left\{ \frac{c_2\sigma z_*^2}{y_*y} + \frac{\alpha\alpha_2 x_* z_*}{(\gamma+x_*)y_*y} \right\} \right. \\ &\quad \left. + \frac{1}{2} \frac{\alpha\alpha_1\alpha_2\gamma z_*}{(\gamma+x)^2(\gamma+x_*)y} \left(1 - \frac{\alpha\gamma}{\gamma+x_*} \right) + \frac{1}{4} \frac{\alpha\alpha_1^2\gamma}{(\gamma+x)^2(\gamma+x_*)} \left(1 - \frac{\alpha\gamma}{\gamma+x_*} \right) \right. \\ &\quad \left. + \frac{1}{4} \frac{\alpha\gamma}{(\gamma+x)^2(\gamma+x_*)} \left\{ \alpha_1^2 - \frac{\alpha\alpha_2^2\gamma z_*^2}{(\gamma+x_*)y^2} \right\} \right] > 0. \end{aligned}$$

Now for \mathbb{P}_3 , we have

$$\begin{aligned} &\Omega_{12}\Omega_{13} - \Omega_{11}\Omega_{23} \\ &= \frac{1}{4} \left[\left\{ \frac{\alpha_1}{(\gamma+x)} - \frac{\alpha\alpha_1\gamma}{(\gamma+x)(\gamma+x_*)} - \frac{\alpha\alpha_2\gamma z_*}{(\gamma+x)(\gamma+x_*)y} \right\} \right. \\ &\quad \times \frac{\alpha_2}{(\gamma+x)} - 2 \left\{ \frac{r}{k} - \frac{(\alpha_1 y_* + \alpha_2 z_*)}{(\gamma+x)(\gamma+x_*)} \right\} \\ &\quad \times \left\{ \sigma(1-c_1) + \sigma\beta(1-c_2) - c_2\sigma \frac{z}{y} - c_2\sigma \frac{z_*}{y} - \frac{\alpha\alpha_2 x}{(\gamma+x)y} \right\} \Big] \\ &= \frac{1}{4} \left[\left\{ \frac{\alpha_2}{(\gamma+x)} \left(\frac{\alpha_1}{(\gamma+x)} - \frac{\alpha\alpha_1\gamma}{(\gamma+x)(\gamma+x_*)} \right. \right. \right. \\ &\quad \left. \left. - \frac{\alpha\alpha_2\gamma z_*}{(\gamma+x)(\gamma+x_*)y} \right) - \frac{2r}{k} \left(\sigma(1-c_1) + \sigma\beta(1-c_2) \right) \right\} \\ &\quad + 2\{\sigma(1-c_1) + \sigma\beta(1-c_2)\} \frac{\alpha_1 y_* + \alpha_2 z_*}{(\gamma+x)(\gamma+x_*)} + 2 \left\{ \frac{r}{k} - \frac{\alpha_1 y_* + \alpha_2 z_*}{(\gamma+x)(\gamma+x_*)} \right\} \\ &\quad \times \left[c_2\sigma \frac{z}{y} + c_2\sigma \frac{z_*}{y} + \frac{\alpha\alpha_2 x}{(\gamma+x)y} \right] \Big] \\ &= \frac{1}{4} \left[\left\{ \frac{\alpha_2}{(\gamma+x)} \left(\frac{\alpha_1}{(\gamma+x)} - \frac{\alpha\alpha_1\gamma}{(\gamma+x)(\gamma+x_*)} - \frac{\alpha\alpha_2\gamma z_*}{(\gamma+x)(\gamma+x_*)y} \right) \right. \right. \\ &\quad \left. \left. - \frac{2r}{k} \left(\sigma(1-c_1) + \sigma\beta(1-c_2) \right) \right\} + 2\{\sigma(1-c_1) \right. \\ &\quad \left. + \sigma\beta(1-c_2)\} \frac{\alpha_1 y_* + \alpha_2 z_*}{(\gamma+x)(\gamma+x_*)} + 2 \left\{ \frac{r}{k} - \frac{\alpha_1 y_* + \alpha_2 z_*}{\gamma(\gamma+x_*)} \right\} \right. \\ &\quad \left. \times \left[c_2\sigma \frac{z}{y} + c_2\sigma \frac{z_*}{y} + \frac{\alpha\alpha_2 x}{(\gamma+x)y} \right] \right] > 0 \text{ (Using (4.3) and (4.4)).} \end{aligned}$$

From (4.5), we have $\Omega_{23} = \frac{1}{2} \{ \sigma(1-c_1) + \sigma\beta(1-c_2) - c_2\sigma \frac{z}{y} - c_2\sigma \frac{z_*}{y} - \frac{\alpha\alpha_2 x}{(\gamma+x)y} \} > 0$.
Using (4.4) and (4.6), for \mathbb{P}_3 , we get

$$\begin{aligned} \Omega_{12}\Omega_{23} - \Omega_{22}\Omega_{13} &= \frac{1}{4} \left[\left\{ \frac{\alpha_1}{(\gamma+x)} - \frac{\alpha\alpha_1\gamma}{(\gamma+x)(\gamma+x_*)} - \frac{\alpha\alpha_2\gamma z_*}{(\gamma+x)(\gamma+x_*)y} \right\} \right. \\ &\quad \times \left\{ \sigma(1-c_1) + \sigma\beta(1-c_2) - c_2\sigma \frac{z}{y} - c_2\sigma \frac{z_*}{y} - \frac{\alpha\alpha_2 x}{(\gamma+x)y} \right\} \\ &\quad \left. - \left\{ \sigma(1-c_1)\beta + \frac{c_2\sigma z^{*2}}{y_*y} + \frac{\alpha\alpha_2 x_* z_*}{(\gamma+x_*)y_*y} \right\} \frac{2\alpha_2}{(\gamma+x)} \right] \\ &= \frac{1}{4} \left[\left\{ \left(\sigma(1-c_1) + \sigma\beta(1-c_2) \right) \right. \right. \\ &\quad \times \left(\frac{\alpha_1}{(\gamma+x)} - \frac{\alpha\alpha_1\gamma}{(\gamma+x)(\gamma+x_*)} - \frac{\alpha\alpha_2\gamma z_*}{(\gamma+x)(\gamma+x_*)y} \right) \\ &\quad \left. \left. - \left(\sigma(1-c_1)\beta + \frac{c_2\sigma z^{*2}}{y_*y} + \frac{\alpha\alpha_2 x_* z_*}{(\gamma+x_*)y_*y} \right) \frac{2\alpha_2}{(\gamma+x)} \right\} \right] \end{aligned}$$

$$\begin{aligned}
 &+ \left\{ c_2\sigma \frac{z}{y} + c_2\sigma \frac{z_*}{y} \right\} \times \left\{ \frac{\alpha\alpha_2\gamma z_*}{(\gamma+x)(\gamma+x_*)y} - \frac{\alpha_1}{(\gamma+x)} \right\} \\
 &+ \frac{\alpha\alpha_2x}{(\gamma+x)y} \left\{ \frac{\alpha\alpha_2\gamma z_*}{(\gamma+x)(\gamma+x_*)y} - \frac{\alpha_1}{(\gamma+x)} \right\} \\
 &+ \frac{\alpha\alpha_1\gamma}{(\gamma+x)(\gamma+x_*)} \left\{ c_2\sigma \frac{z}{y} + c_2\sigma \frac{z_*}{y} + \frac{\alpha\alpha_2x}{(\gamma+x)y} \right\} \Big] > 0
 \end{aligned}$$

Above results suggest that $\mathbb{P}_3 > 0$, so the conditions (i), (ii) and (iii) imply that $\dot{\Sigma} < 0$ along the trajectories. Therefore, system (2.4) is globally stable around the interior equilibrium point B_* according as the conditions stated in the theorem hold.

Appendix 2

Let $\mu(\sigma) = \varrho(\sigma) + i\zeta(\sigma)$ for all $\sigma \in R^+$, the characteristic value of the characteristic Eq. (7.1). Substituting this value in Eq. (7.1), and separate real and imaginary parts as

$$\varrho^3 - 3\varrho\zeta^2 + (\varrho^2 - \zeta^2)\Theta_1 + \varrho\Theta_2 + \Theta_3 = 0, \tag{7.2}$$

$$3\varrho^2\zeta - \zeta^3 + 2\varrho\zeta\Theta_1 + \zeta\Theta_2 = 0. \tag{7.3}$$

A necessary condition for a Hopf bifurcation of B_* is that the characteristic equation (7.1) should have purely imaginary solutions. For the Hopf bifurcation to occur at $\sigma = \sigma^*$, substituting $\Theta_1(\sigma^*)\Theta_2(\sigma^*) = \Theta_3(\sigma^*)$ into Eq. (7.1), the characteristic equation must be of the form

$$[\mu^2 + \Theta_2(\sigma^*)][\mu + \Theta_1(\sigma^*)] = 0. \tag{7.4}$$

Thus, the characteristic values of the Eq. (7.4) are $\mu_{1,2}(\sigma^*) = \pm i\sqrt{\Theta_2(\sigma^*)} = \pm i\zeta^*$ and $\mu_3(\sigma^*) = -\Theta_1(\sigma^*)$. By using the condition (i) of the Theorem 4, we have $\zeta^* > 0$ and $\mu_3(\sigma^*) < 0$.

Now, we can verify the transversality condition

$$\left[\frac{d}{d\sigma} [Re\{\mu(\sigma)\}] \right]_{\sigma=\sigma^*} \neq 0. \tag{7.5}$$

Calculating the derivative of (7.2) and (7.3) w.r.t. σ and substituting $\varrho = 0, \zeta = \zeta^*$ and $\sigma = \sigma^*$, we get

$$\begin{aligned}
 \mathcal{P} \left[\frac{d[Re\{\mu(\sigma)\}]}{d\sigma} \right]_{\sigma=\sigma^*} - \mathcal{Q} \left[\frac{d[Im\{\mu(\sigma)\}]}{d\sigma} \right]_{\sigma=\sigma^*} &= \mathcal{L}, \\
 \mathcal{Q} \left[\frac{d[Re\{\mu(\sigma)\}]}{d\sigma} \right]_{\sigma=\sigma^*} + \mathcal{P} \left[\frac{d[Im\{\mu(\sigma)\}]}{d\sigma} \right]_{\sigma=\sigma^*} &= \mathcal{M},
 \end{aligned} \tag{7.6}$$

where $\mathcal{P} = -2\Theta_2(\sigma^*), \mathcal{Q} = 2\Theta_1(\sigma^*)\sqrt{\Theta_2(\sigma^*)}, \mathcal{L} = \dot{\Theta}_1(\sigma^*)\Theta_2(\sigma^*) - \dot{\Theta}_3(\sigma^*), \mathcal{M} = -\dot{\Theta}_2(\sigma^*)\sqrt{\Theta_2(\sigma^*)}$.

Solving for $\dot{\mu}(\sigma^*)$ from system (7.6) we obtained

$$\begin{aligned} \left[\frac{d}{d\sigma} [Re\{\mu(\sigma)\}] \right]_{\sigma=\sigma^*} &= \dot{\mu}(\sigma^*) = \frac{\mathcal{L}\mathcal{P} + \mathcal{M}\mathcal{Q}}{\mathcal{P}^2 + \mathcal{Q}^2} \\ &= \frac{2\Theta_2(\sigma^*)\{\dot{\Theta}_3(\sigma^*) - \Theta_1(\sigma^*)\dot{\Theta}_2(\sigma^*) - \dot{\Theta}_1(\sigma^*)\Theta_2(\sigma^*)\}}{\mathcal{P}^2 + \mathcal{Q}^2}. \end{aligned}$$

Hence $\dot{\mu}(\sigma^*) > 0$, if $\Theta_2(\sigma^*) > 0$ and $\dot{\Theta}_3(\sigma^*) > [\Theta_1(\sigma^*)\Theta_2(\sigma^*)]'$. Therefore, the transversality condition is satisfied and a Hopf bifurcation occurs when σ passes through the critical value σ^* .

Appendix 3

Let \tilde{p} be a point in the positive quadrant and $o(\tilde{p})$ be orbit through \tilde{p} and $\tilde{\Omega}(\tilde{p})$ be the bounded omega limit set of the orbit through \tilde{p} . $W^s(B_r)$ denotes the stable manifold of B_r , $r = 1, 2$.

Clearly $B_0 \notin \tilde{\Omega}(\tilde{p})$. If possible, let $B_0 \in \tilde{\Omega}(\tilde{p})$ then by the *Butler-McGehee* lemma there exists a point m in $\tilde{\Omega}(\tilde{p}) \cap W^s(B_0)$. But, $o(m)$ lies in $\tilde{\Omega}$ and $W^s(B_0)$ is the yz -plane, which shows that $o(m)$ is unbounded, a contradiction.

Next we show that $B_1 \notin \tilde{\Omega}(\tilde{p})$. If $B_1 \in \tilde{\Omega}(\tilde{p})$, the condition $R_{01} > 1$ implies that B_1 is a saddle point, then applying the *Butler-McGehee* lemma there exists a point m in $\tilde{\Omega}(\tilde{p}) \cap W^s(B_1)$. Now $\tilde{\Omega}(\tilde{p}) \cap W^s(B_1)$ is the xz -space and hence orbit in this plane emanate from either B_1 or an unbounded orbit lies in $\tilde{\Omega}(\tilde{p})$, which is a contradiction.

Finally, we show that no periodic orbit solution in the xy -space or $B_2 \in \tilde{\Omega}(\tilde{p})$. If q_j , $j = 1, 2, \dots, n$ denote the closed orbit of the periodic solution $(\varphi_q(t), \psi_q(t))$ in xy -space such that q_j lies inside q_{j-1} . Let, the Jacobian matrix J of the system (2.4) corresponding to q_j be denoted by $J_q(\varphi_q(t), \psi_q(t), 0)$. The fundamental matrix of the linear periodic system is given by

$$\dot{Z} = J_q(t), \quad Z(0) = Z_0. \tag{7.7}$$

We find that, $e^{\xi_q T}$ is the Floquet multiplier of (7.7) in the direction of z . Then applying the process as proposed by Kumar and Freedman (1989), we conclude that no q_j lies on $\tilde{\Omega}$. Therefore, $\tilde{\Omega}$ lies in the positive quadrant and system (2.4) is persistent. Since only the closed orbits and the equilibria from the omega limit set of the solutions are on the boundary of R^3_+ and system (2.4) is dissipative. Thus, the system (2.4) is uniformly persistent by the main theorem of Butler et al. (1986).

References

1. Anderson, R.M., May, R.M.: The invasion, persistence and spread of infectious diseases within animal and plant communities. *Philos. Trans. R. Soc. Lond. B Biol. Sci.* **314**, 533–570 (1986)
2. Biswas, S., Samanta, S., Chattopadhyay, J.: Cannibalistic predator–prey model with disease in predator—a delay model. *Int. J. Bif. Chaos* **25**(10), 1550130 (2015)

3. Biswas, S., Chatterjee, S., Chattopadhyay, J.: Cannibalism may control disease in predator population: result drawn from a model based study. *Math. Methods Appl. Sci.* **38**, 2272–2290 (2015)
4. Biswas, S., Samanta, S., Chattopadhyay, J.: A model based theoretical study on cannibalistic prey–predator system with disease in both populations. *Differ. Equ. Dyn. Syst.* **23**(3), 327–370 (2015)
5. Biswas, S., Samanta, S., Khan, Q.J., Chattopadhyay, J.: Effect of multiple delays on the dynamics of cannibalistic prey–predator system with disease in both populations. *Int. J. Biomath.* (2016). doi:[10.1142/S1793524517500498](https://doi.org/10.1142/S1793524517500498)
6. Boots, M.: Cannibalism and the stage-dependent transmission of a viral pathogen of the Indian meal moth, *Plodia interpunctella*. *Ecol. Entomol.* **23**, 118–122 (1998)
7. Butcher, J.C.: Coefficients for the study of Runge–Kutta integration processes. *J. Aust. Math. Soc.* **3**(02), 185–201 (1963)
8. Chapman, J.W., Williams, T., Escribano, A., Caballero, P., Cave, R.D., Goulson, D.: Fitness consequence of cannibalism in the fall armyworm, *Spodoptera frugiperda*. *Behav. Ecol.* **10**, 298–303 (1998)
9. Chapman, J.W., Williams, T., Escribano, A., Caballero, P., Cave, R.D., Goulson, D.: Age-related cannibalism and horizontal transmission of a nuclear polyhedrosis virus in larval *Spodoptera frugiperda*. *Ecol. Entomol.* **24**, 268–275 (1999)
10. Chattopadhyay, J., Arino, O.: A predator–prey model with disease in the prey. *Nonlinear Anal.* **36**, 747–766 (1999)
11. Cushing, J.M.: A simple model of cannibalism. *Math. Biosci.* **107**, 47–71 (1991)
12. Das, K., Samanta, S., Biswas, B., Chattopadhyay, J.: Occurrence of chaos and its possible control in a predator–prey model with disease in the predator population. *J. Ecol.* **108**, 306–319 (2014)
13. Das, K.P., Samanta, S., Biswas, S., Alshomrani, A.S., Chattopadhyay, J.: A strategy for a disease-free system—an eco-epidemiological model based study. *J. Appl. Math. Comput.* (2016). doi:[10.1007/s12190-016-1050-7](https://doi.org/10.1007/s12190-016-1050-7)
14. Desharnais, R.A., Liu, L.: Stable demographic limit cycles in laboratory populations of *Tribolium castaneum*. *J. Anim. Ecol.* **56**, 885–906 (1987)
15. Diekmann, O., Nibet, R.M., Gurney, W.S.C., Van den Bosch, F.: Simple mathematical models for cannibalism: a critique and a new approach. *Math. Biosci.* **78**, 21–46 (1986)
16. Elgar, M.A., Crespi, B.J.: *Cannibalism: Ecology and Evolution Among Diverse Taxa*. Oxford University Press, New York (1992)
17. Evirgen, F., Özdemir, N.: Multistage adomian decomposition method for solving NLP problems over a nonlinear fractional dynamical system. *J. Comput. Nonlinear Dyn.* **6**(2), 021003 (2011)
18. Fatoorehchi, H., Abolghasemi, H., Zarghami, R.: Analytical approximate solutions for a general nonlinear resistor–nonlinear capacitor circuit model. *Appl. Math. Model.* **39**(19), 6021–6031 (2015)
19. Fatoorehchi, H., Abolghasemi, H., Zarghami, R., Rach, R.: Feedback control strategies for a cerium-catalyzed Belousov–Zhabotinsky chemical reaction system. *Can. J. Chem. Eng.* **93**(7), 1212–1221 (2015)
20. Fatoorehchi, H., Zarghami, R., Abolghasemi, H., Rach, R.: Chaos control in the cerium-catalyzed Belousov–Zhabotinsky reaction using recurrence quantification analysis measures. *Chaos Solitons Fract.* **76**, 121–129 (2015)
21. Fox, L.R.: Cannibalism in natural populations. *Annu. Rev. Ecol. Syst.* **6**, 87–106 (1975)
22. Fraser, C.A., Owens, L.: Spawner-isolated mortality virus from Australian *Penaeus monodon*. *Dis. Aquat. Org.* **27**, 141–148 (1996)
23. Godfray, H.C.J.: *Parasitoids: Behavioral and Evolutionary Ecology*. Princeton University Press, Princeton (1994)
24. Greenhalgh, D., Haque, M.: A predator–prey model with disease in the prey species only. *Math. Methods Appl. Sci.* **30**, 911–929 (2007)
25. Guthrie, D.M., Tindall, A.R.: *The Biology of the Cockroach*. St. Martins Press, New York (1968)
26. Haderler, K.P., Freedman, H.I.: Predator–prey populations with parasitic infection. *J. Math. Biol.* **27**, 609–631 (1989)
27. Haque, M., Venturino, E.: The role of transmissible diseases in the Holling–Tanner predator–prey model. *Theor. Pop. Biol.* **70**, 273–288 (2006)
28. Haque, M., Venturino, E.: An ecoepidemiological model with disease in predator: the ratio-dependent case. *Math. Methods Appl. Sci.* **30**, 1791–1809 (2007)
29. Haque, M.: A predator–prey model with disease in the predator species only. *Nonlinear Anal. Real World Appl.* **11**, 2224–2236 (2010)
30. Hastings, A.: Cycles in cannibalistic egg–larval interactions. *J. Math. Biol.* **24**, 651–666 (1987)

31. Hethcote, H.W., Wang, W., Han, L., Ma, Z.: A predator–prey model with infected prey. *Theor. Popul. Biol.* **66**(3), 249–268 (2004)
32. Hilker, F.M., Schmitz, K.: Disease-induced stabilization of predator–prey oscillations. *J. Theor. Biol.* **255**, 299–306 (2008)
33. Hofbauer, J.: Saturated equilibria, permanence and stability for ecological systems. In: Groos, L., Hallam, T., Levin, S. (eds.) *Proceedings of the 2nd Autumn Course on Mathematical Ecology*. World Scientific, Trieste (1986)
34. Holmes, N.D., Nelson, W.A., Peterson, L.K., Farstad, C.W.: Causes of variations in effectiveness of *Bracon cephi* (Gahan) (Hymenoptera: Braconidae) as a parasite of the wheat stem sawfly. *Can. Entomol.* **95**, 113–126 (1963)
35. Hutson, V., Law, R.: Permanent coexistence in general models of three interacting species. *J. Math. Biol.* **21**(3), 285–298 (1985)
36. Ibáñez, C.M., Chong, J.: Feeding ecology of *Enteroctopus megalocyathus* (Gould 1852) (Cephalopoda: Octopodidae). *J. Mar. Biol. Assoc. UK* **88**, 793–798 (2008)
37. Ibanez, C.M., Keyal, F.: Cannibalism in cephalopods. *Rev. Fish Biol. Fish.* (2009). doi:[10.1007/s11160-009-9129-y](https://doi.org/10.1007/s11160-009-9129-y)
38. Jancovich, J.K., Daviodson, E.W., Morado, J.F., Jacobs, B.L., Colling, J.P.: Isolation of a lethal virus from the endangered tiger salamander *Ambystoma tigrinum stebbinsi*. *Dis. Aquatic Org.* **31**, 161–167 (1997)
39. Kohlmeier, C., Ebenhoj, W.: The stabilizing role of cannibalism in a predator–prey system. *Bull. Math. Biol.* **57**, 401–411 (1995)
40. Magnússon, K.G.: Destabilizing effect of cannibalism on a structured predator–prey system. *Math. Biosci.* **155**, 61–75 (1999)
41. Richardson, M.L., Mitchell, R.F., Reagel, P.F., Hanks, L.M.: Causes and consequences of cannibalism in noncarnivorous insects. *Annu. Rev. Entomol.* **55**, 39–53 (2010)
42. Pfennig, D.W., Loeb, M.L.G., Collins, J.P.: Pathogens as a factor limiting the spread of cannibalism in tiger salamanders. *Oecologia* **88**, 161–166 (1991)
43. Pielou, E.C.: *Introduction to Mathematical Ecology*. Wiley-Interscience, New York (1969)
44. Polis, G.A.: The evolution and dynamics of intraspecific predation. *Annu. Rev. Ecol. Syst.* **12**, 225–251 (1981)
45. Ré, M.E., Gomez-Simes, E.: Hábitos alimentarios del pulpo (*Octopus tehuelchus*). I. Analisis cualitativo de la dieta en el intermareal de Puerto Lobos, Golfo San Matías (Argentina). *Frente Marítimo* **11**: 119–128 (1992)
46. Root, R.B., Chaplin, S.J.: The life-styles of tropical milkweed bugs, *Oncopeltus* (Hemiptera: Lygaeidae), utilizing the same hosts. *Ecology* **57**, 132–140 (1976)
47. Root, R.B.: The life of a Californian population of the facultative milkweed bug *Lygaeus kalmii* (Heteroptera: Lygaeidae). *Proc. Entomol. Soc. Wash.* **88**, 201–214 (1986)
48. Rosenzweig, M.L., MacArthur, R.H.: Graphical representation and stability conditions of predator-prey interactions. *Am. Nat.* **97**, 209–223 (1963)
49. Rudolf, V.H.W., Antonovics, J.: Disease transmission by cannibalism: rare event or common occurrence? *Proc. R. Soc. B* **274**, 1205–1210 (2007)
50. Saifuddin, M., Biswas, S., Samanta, S., Sarkar, S., Chattopadhyay, J.: Complex dynamics of an eco-epidemiological model with different competition coefficients and weak Allee in the predator. *Chaos Solitons Fract.* **91**, 270–285 (2016)
51. Samanta, S., Dhar, R., Pal, J., Chattopadhyay, J.: Effect of enrichment on plankton dynamics where phytoplankton can be infected from free viruses. *Nonlinear Stud.* **20**(2), 225–238 (2013)
52. Samanta, S., Mandal, A.K., Kundu, K., Chattopadhyay, J.: Control of disease in prey population by supplying alternative food to predator. *J. Biol. Syst.* **22**(04), 677–690 (2014)
53. Spann, K.M., Cowley, J.A., Walker, P.J., Lester, R.J.G.: A yellow head-like virus, from *Penaeus monodon* cultured in Australia. *Dis. Aquat. Org.* **31**, 169–179 (1997)
54. Van den Bosch, F., Gabriel, W.: Cannibalism in an age-structured predator–prey system. *Bull. Math. Biol.* **59**, 551–567 (1997)
55. Venturino, E.: The influence of diseases on Lotka–Volterra systems. *Rocky Mt. J. Math.* **24**, 381–402 (1994)
56. Venturino, E.: Epidemics in predator–prey models: disease in the prey. In: Arino, O., Axelrod, D., Kimmel, M., Langlais, M. (eds.) *Mathematical Population Dynamics: Analysis of Heterogeneity*, vol. 1: Theory of Epidemics, pp. 381–393. Wuerz Publishing, Winnipeg (1995)

57. Venturino, E.: Epidemics in predator–prey models: disease in the predators. *IMA J. Math. Appl. Med. Biol.* **19**, 185–205 (2002)
58. Weaver, D.K., Nansen, C., Runyon, J.B., Sing, S.E., Morrill, W.L.: Spatial distributions of *Cephus cinctus* Norton (Hymenoptera: Cephidae) and its braconid parasitoids in Montana wheat fields. *Biol. Control* **34**, 1–11 (2005)
59. Wood, J.B., Kenchington, E., O’Dor, R.K.: Reproduction and embryonic development time of *Bathypolypus articus*, a deep-sea octopod (Cephalopoda: Octopoda). *Malacologia* **39**, 11–19 (1998)
60. Yang, X., Chen, L.S.: Permanence and positive periodic solution for the single species nonautonomous delay diffusive model. *Comp. Math. Appl.* **32**, 109–116 (1996)
61. Ziemba, R.E., Collins, J.P.: Development size structure in tiger salamanders: the role of intraspecific interference. *Oecologia* **120**, 524–529 (1999)